N-alkylpiperidine carbamates as potential anti-Alzheimer's agents

Urban Košak, Nika Strašek, Damijan Knez, Marko Jukič, Simon Žakelj, Abida Zahirović, Anja Pišlar, Xavier Brazzolotto, Florian Nachon, Janko Kos, Stanislav Gobec

PII: S0223-5234(20)30251-8

DOI: https://doi.org/10.1016/j.ejmech.2020.112282

Reference: EJMECH 112282

To appear in: *European Journal of Medicinal Chemistry*

Received Date: 27 February 2020

Revised Date: 26 March 2020

Accepted Date: 26 March 2020

Please cite this article as: U. Košak, N. Strašek, D. Knez, M. Jukič, S. Žakelj, A. Zahirović, A. Pišlar, X. Brazzolotto, F. Nachon, J. Kos, S. Gobec, N-alkylpiperidine carbamates as potential anti-Alzheimer's agents, *European Journal of Medicinal Chemistry* (2020), doi: https://doi.org/10.1016/j.ejmech.2020.112282.

Compound structure and number	hAChE inhibition	hBChE inhibition	hMAO-B inhibition	BBB permeable	Inhibition of $A\beta_{1-42}$ aggregation	Non-cytotoxic	Neuro-protective
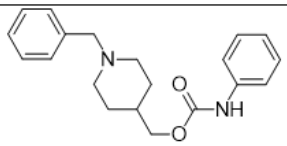 **10**	✓	✓	✓	✓	✗	✓	✓
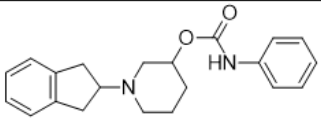 **13**	✗	✓	✗	✓	✗	✓	✗
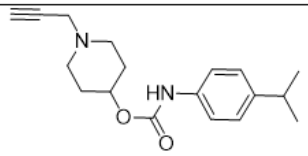 **16**	✗	✗	✓	✓	✓	✓	✓
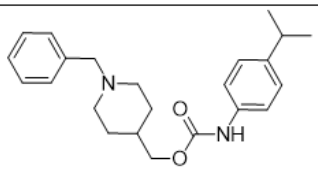 **22**	✓	✓	✗	✓	✗	✓	✗

N-alkylpiperidine carbamates as potential anti-Alzheimer's agents

*Urban Košak,[‡] Nika Strašek,[‡] Damijan Knez,[‡] Marko Jukič,[‡] Simon Žakelj,[‡] Abida Zahirović,[‡] Anja Pišlar,[‡] Xavier Brazzolotto,[ø] Florian Nachon,[ø] Janko Kos,[‡] Stanislav Gobec[‡,]**

[‡] University of Ljubljana, Faculty of Pharmacy, Aškerčeva 7, 1000 Ljubljana, Slovenia

[ø] Institut de Recherche Biomédicale des Armées, 91223 Brétigny-sur-Orge, France

***Corresponding Author:** Stanislav Gobec

University of Ljubljana, Faculty of Pharmacy, Aškerčeva 7, 1000 Ljubljana, Slovenia

Tel: +386-1-4769500; Fax: +386-1-4258031; E-mail: stanislav.gobec@ffa.uni-lj.si

Abstract

Compounds capable of interacting with single or multiple targets involved in Alzheimer's disease (AD) pathogenesis are potential anti-Alzheimer's agents. In our aim to develop new anti-Alzheimer's agents, a series of 36 new *N*-alkylpiperidine carbamates was designed, synthesized and evaluated for the inhibition of cholinesterases [acetylcholinesterase (AChE) and butyrylcholinesterase (BChE)] and monoamine oxidases [monoamine oxidase A (MAO-A and monoamine oxidase B (MAO-B)]. Four compounds are very promising: multiple AChE (IC_{50} = 7.31 µM), BChE (IC_{50} = 0.56 µM) and MAO-B (IC_{50} = 26.1 µM) inhibitor **10**, dual AChE (IC_{50} = 2.25 µM) and BChE (IC_{50} = 0.81µM) inhibitor **22**, selective BChE (IC_{50} = 0.06 µM) inhibitor **13**, and selective MAO-B (IC_{50} = 0.18 µM) inhibitor **16**. Results of enzyme kinetics experiments showed that despite the carbamate group in the structure, compounds **10**, **13**, and **22** are reversible and non-time-dependent inhibitors of AChE and/ or BChE. The resolved crystal structure of the complex of BChE with compound **13** confirmed the non-covalent mechanism of inhibition. Additionally, *N*-propargylpiperidine **16** is an irreversible and time-dependent inhibitor of MAO-B, while *N*-benzylpiperidine **10** is reversible. Additionally, compounds **10**, **13**, **16**, and **22** should be able to cross the blood-brain barrier and are not cytotoxic to human neuronal-like SH-SY5Y and liver HepG2 cells. Finally, compounds **10** and **16** also prevent amyloid β_{1-42} ($A\beta_{1-42}$)-induced neuronal cell death. The neuroprotective effects of compound **16** could be the result of its $A\beta_{1-42}$ anti-aggregation effects.

Keywords

Alzheimer's disease; Acetylcholinesterase; Butyrylcholinesterase; Monoamine oxidase; Multi-target-directed ligands; *N*-alkylpiperidine carbamates.

1. Introduction

Alzheimer's disease (AD) is a neurodegenerative brain disease[1] with amyloid β peptide (Aβ) deposits (amyloid plaques),[2] and products of oxidative stress[3] contributing to the pathogenesis of the disease. Amyloid plaques are mainly composed of a 42-amino-acid-long Aβ isoform ($A\beta_{1-42}$)[4], which forms cytotoxic structures, ranging from monomers to oligomers (i.e., 2–6 monomers) and fibers[2,5]. Several small molecules [e.g. elenbecestat (E2609), umibecestat (CNP520)] and macromolecules (e.g. gantenerumab, CAD106, UB-311) targeting the production and clearance of Aβ monomers, oligomers and fibres are currently evaluated in clinical trials for the treatment of AD[6,7].

One of the several proteins that contribute to oxidative stress in AD is monoamine oxidase (MAO)[8], a flavin adenine dinucleotide (FAD)-containing enzyme located in the outer mitochondrial membrane that catalyses the oxidative deamination of monoamines[9]. MAO-A and MAO-B are the two isoenzymes present in most mammalian tissues[8]. The enzymatic activity of MAO-B is increased in the brains of patients with AD[8,9]. This results in increased levels of oxidative deamination reaction products such as hydrogen peroxide, a source of hydroxyl radicals, aldehydes and ammonia[8–10]. These products contribute to oxidative stress[8], which enhances the neurodegeneration and synaptic dysfunction in AD[2]. For example, selective MAO-B inhibitor rasagiline (Figure 1) is currently evaluated in a phase II clinical trial for the treatment of AD[7].

The neurodegeneration and synaptic dysfunction in AD severely affect the cholinergic system[11] and result in a decrease in the levels of the neurotransmitter acetylcholine (ACh)[12], which then produces memory loss and cognitive impairment[13], distinctive for patients with AD. Acetylcholinesterase (AChE) and butyrylcholinesterase (BChE) are the two cholinesterases (ChEs) that terminate cholinergic neurotransmission by catalysing the hydrolysis of ACh[14]. Inhibition of ACh hydrolysis in the brain is used to increase levels of

ACh and consequently restore cognitive functions and alleviate symptoms of AD[15]. Accordingly, three out of the four approved drugs for alleviating symptoms of AD are ChE inhibitors[16]: selective AChE inhibitors donepezil[17] and galantamine[18], and dual ChE inhibitor rivastigmine[19] (Figure 1).

Considering the intricate nature of AD pathogenesis, the multitarget-directed ligand (MTDL) approach has also been used to develop compounds capable of interacting with more than one target involved in the pathogenesis of the disease[20–22]. For example, multitarget compounds ladostigil (inhibition of AChE, BChE, MAO-A, and MAO-B)[23] and AD-35 (inhibition of AChE and metal-induced Aβ aggregation)[24] (Figure 1) are currently evaluated in a phase II clinical trial[25,7].

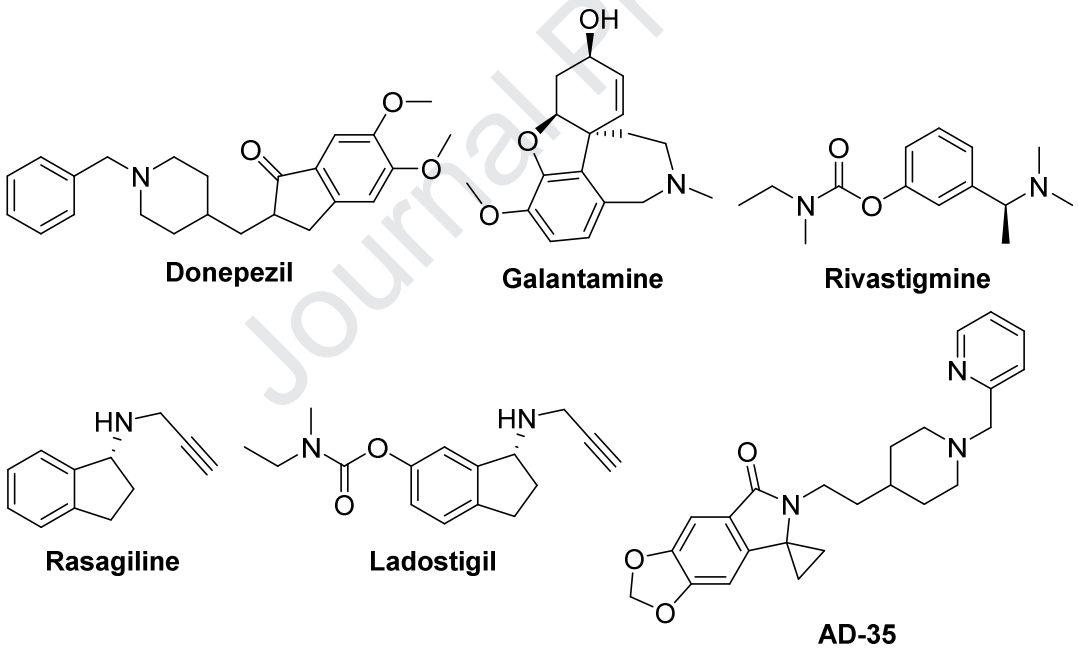

Figure 1. Structures of the currently approved ChE inhibitors for the treatment of Alzheimer's disease (donepezil, galantamine, and rivastigmine), and structures of some of the compounds currently evaluated in clinical trials for the treatment of AD (rasagiline, ladostigil and AD-35).

Among all therapeutic areas, AD has one of the lowest numbers of compounds progressing to regulatory review. No new drugs have been approved since 2003, and the overall success rate during the 2002 to 2012 period was only 0.4%. This very high attrition rate (99.6%) requires a constant supply of new compounds that can be evaluated for efficacy in AD[26]. In the current study, our hypothesis was that novel anti-AD compounds, capable of interacting with one or more targets in AD pathogenesis, can be developed simply by combining moieties of known anti-AD compounds. We report herein design, straightforward two-step synthesis, and comprehensive biochemical evaluation of a series of *N*-alkylpiperidine carbamates as potential anti-Alzheimer agents.

2. Results and discussion

2.1. Design

N-Alkylpiperidine carbamates were designed by fusing moieties of known ChE and MAO-B inhibitors (Figure 2). The 1,3- and 1,4-disubstituted piperidine scaffold, the hallmark of the series, was taken from selective BChE inhibitors with neuroprotective activity **1**[27], **2**[28], and **3**[29], and selective AChE inhibitor donepezil[17]. Compound **1** is a hit compound discovered using a hierarchical structure-based virtual screening protocol to identify novel BChE inhibitors[27]. Compounds **2** and **3** are lead compounds developed in a hit-to-lead optimization campaigns[28,29] using compound **1** as the starting point. The *N*-benzyl group was taken from sulfonamide **2**[28] and donepezil[17], *N*-(2,3-dihydro-1*H*-inden-2-yl) group was appropriated from amides **1**[27] and **3**[29]. Rasagiline is a selective MAO-B inhibitor with neuroprotective activity, which inhibits MAO-B by forming a covalent bond between *N*-propargyl group and the *N*5 atom of FAD cofactor[30]. The *N*-propargyl group of rasagiline was thus introduced to the piperidine nitrogen to design compounds capable of inhibiting ChEs and MAO-B. Dual ChE

inhibitor rivastigmine[19], selective AChE inhibitor phenserine[31] and selective BChE inhibitor bisnorcymserine[32] are pseudo-irreversible ChE inhibitors, which inhibit their target enzymes by carbamoylation of the catalytic serine in the active site of ChEs. The active site is then slowly regenerated by decarbamylation[33]. The carbamate moieties of these three compounds were thus introduced to the 3- or 4- position of piperidine ring directly (n = 0, Figure 2), or *via* a methylene group (n = 1, Figure 2).

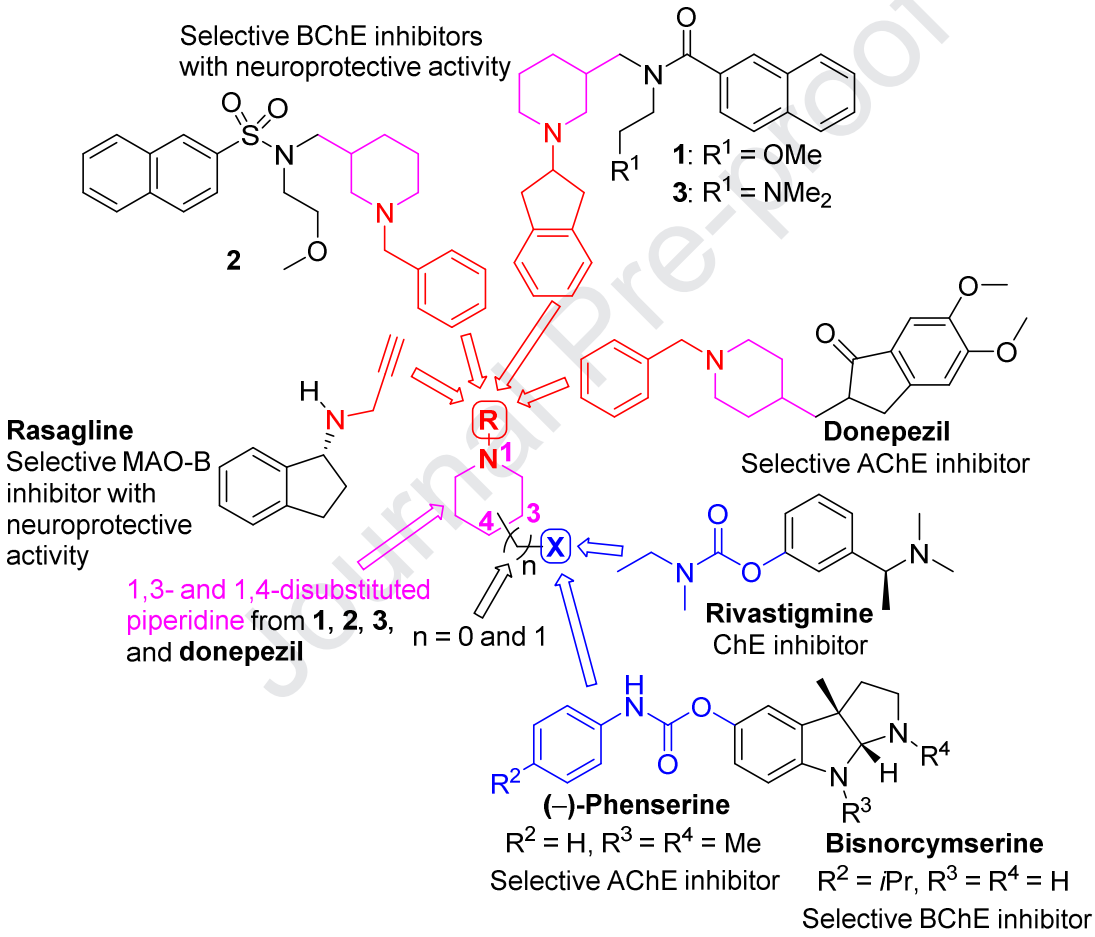

Figure 2. Design of *N*-alkylpiperidine carbamates.

2.2. Synthesis

The synthesis of *N*-alkylpiperidine carbamates **4**–**39** is presented in Table 1. First, the nitrogen of commercially available 4-hydroxypiperdine (**40**), 3-hydroxypiperidine (**41**), 4-

(hydroxymethyl)piperidine (**42**), and 3-(hydroxymethyl)piperidine (**43**) was alkylated with propargyl bromide or benzyl bromide in the presence of Cs_2CO_3 in acetone at room temperature[34], to produce *N*-propargylpiperidine alcohols **44**–**47** and *N*-benzylpiperidine alcohols **48**–**51** in moderate to high yields (63–88%). *N*-(2,3-dihydro-1*H*-inden-2-yl) piperidine alcohols **52**–**55** were prepared in modest yields (21–33%) by alkylating the nitrogen of starting piperidines **40**–**43** with 2-bromo-2,3-dihydro-1*H*-indene (**56**) in the presence of K_2CO_3 and a catalytic amount of KI in MeCN at reflux. Bromide **56** was prepared from 2,3-dihydro-1*H*-inden-2-ol (**57**) and bromine in the presence of triphenylphosphine in CH_2Cl_2[35] in 83% yield.

The designed phenyl carbamates **4**–**15** and 4-isopropylphenyl carbamates **16**–**27** were synthesized in high yields (85–96%) by treating *N*-alkyl alcohols **44**–**55** with phenyl isocyanate or 4-isopropylphenyl isocyanate in the presence of a catalytic amount of *N*,*N*-dimethylpyridin-4-amine (4-DMAP) in CH_2Cl_2 at room temperature[36]. Ethyl(methyl) carbamates **28**–**39** were prepared in modest to moderate yields (28–54%) by treating *N*-alkylpiperidine alcohols **44**–**55** with *N*-ethyl-*N*-methylcarbamoyl chloride in pyridine at reflux[37].

Table 1. Synthesis of designed compounds. Reagents and conditions: (a) propargyl bromide (80 wt% solution in PhMe) or benzyl bromide, Cs_2CO_3, acetone, rt, 24 h (82–86%); (b) 2-bromo-2,3-dihydro-1*H*-indene, K_2CO_3, cat. KI, MeCN, reflux (85 °C), 24 h (21–33%); (c) PhNCO or 4-*i*PrPhNCO, cat. 4-DMAP, CH_2Cl_2, rt, 24 h (85–96%); (d) *N*-ethyl-*N*-methylcarbamoyl chloride, pyridine, reflux (120 °C), 24 h (28–54%).

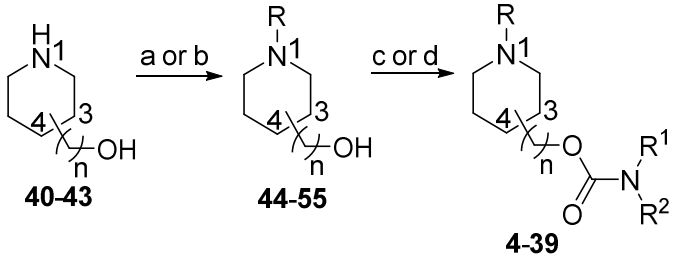

Compds[a]	Pdp[b]	R	n	R^1	R^2	Compds[a]	Pdp[b]	R	n	R^1	R^2
4	1,4		0	H	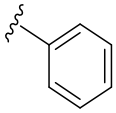	**30**	1,4		1	Me	Et
5	1,3		0	H	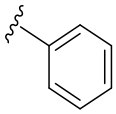	**31**	1,3		1	Me	Et
6	1,4		1	H	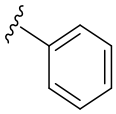	**32**	1,4	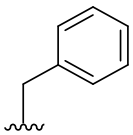	0	Me	Et
7	1,3		1	H	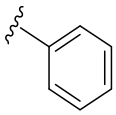	**33**	1,3	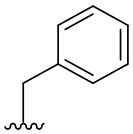	0	Me	Et
8	1,4	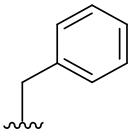	0	H	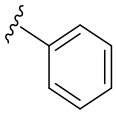	**34**	1,4	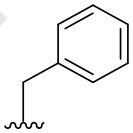	1	Me	Et
9	1,3	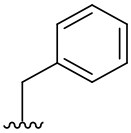	0	H	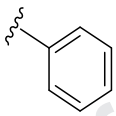	**35**	1,3	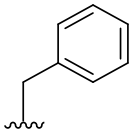	1	Me	Et
10	1,4	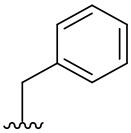	1	H	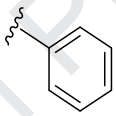	**36**	1,4		0	Me	Et
11	1,3	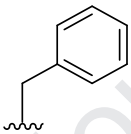	1	H	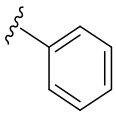	**37**	1,3		0	Me	Et
12	1,4		0	H	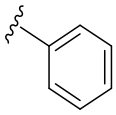	**38**	1,4		1	Me	Et
13	1,3	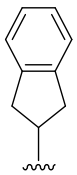	0	H	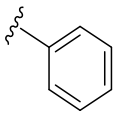	**39**	1,3	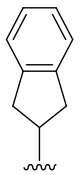	1	Me	Et
14	1,4		1	H	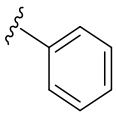	**40**	1,4	/	0	/	/
15	1,3	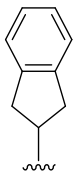	1	H	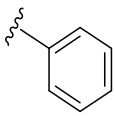	**41**	1,3	/	0	/	/

16	1,4		0	H	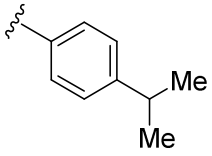	**42**	1,4	/	1	/	/
17	1,3		0	H	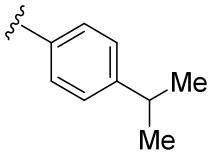	**43**	1,3	/	1	/	/
18	1,4		1	H	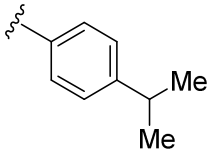	**44**	1,4		0	/	/
19	1,3		1	H	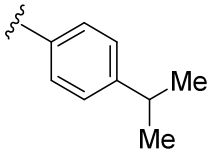	**45**	1,3		0	/	/
20	1,4	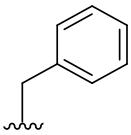	0	H	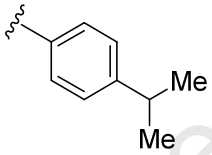	**46**	1,4		1	/	/
21	1,3	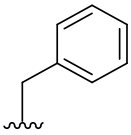	0	H	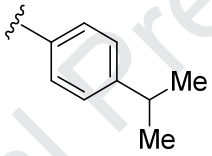	**47**	1,3		1	/	/
22	1,4	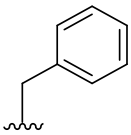	1	H	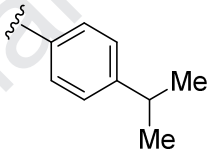	**48**	1,4	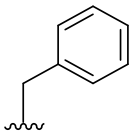	0	/	/
23	1,3	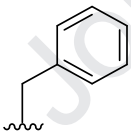	1	H	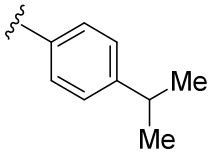	**49**	1,3	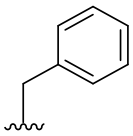	0	/	/
24	1,4		0	H	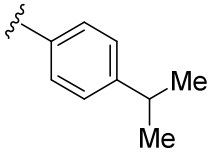	**50**	1,4	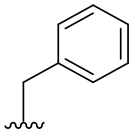	1	/	/
25	1,3		0	H	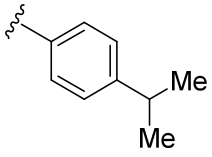	**51**	1,3	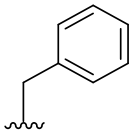	1	/	/
26	1,4	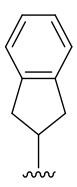	1	H	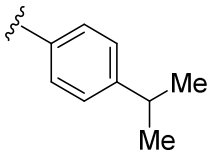	**52**	1,4		0	/	/

27	1,3		1	H	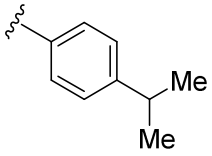	**53**	1,3		0 / /
28	1,4		0	Me	Et	**54**	1,4		1 / /
29	1,3		0	Me	Et	**55**	1,3		1 / /

[a]**Compds** = compound number

[b]**Pdp** = piperidine disubstitution pattern

2.3. *In vitro* enzyme inhibition

The inhibitory potencies against human (h)BChE and hAChE of all synthesized *N*-alkyl piperidines were determined using the method of Ellman[38], and the inhibitory potencies against human (h)MAO-A and hMAO-B were determined using a previously described fluorescence-based Amplex Red assay[39] with minor modifications. Table 2 and Table 3 report the structures and inhibitory potencies of 1,4-disubstituted *N*-alkylpiperidines carbamates and 1,3-disbstituted *N*-alkylpiperidines carbamates, respectively. Compounds with IC_{50} values higher than 100 µM were considered inactive (no inhibition). Since *N*-alkylpiperidine alcohols **44**–**55** did not inhibit (IC_{50} > 100 µM) any of the four enzymes, they have not been included in Table 1. Since none of the compounds inhibited hMAO-A (IC_{50} > 100 µM), these values have not been included in Table 1. Rasagiline and rivastigmine were used as controls for hMAO and hChE inhibition, respectively.

Table 2. Inhibitory potencies and structures of 1,4-disubstituted *N*-alkylpiperidine carbamates.

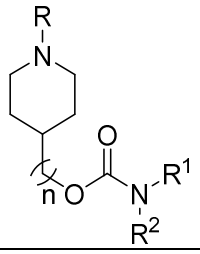

Compds[a]	R	n	R^1	R^2	hAChE[b] IC_{50} ±SEM (μM)	hBChE[b] IC_{50} ±SEM (μM)	hMAO-B[c] IC_{50} ±SEM (μM)
4	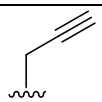	0	H	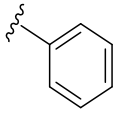	>100	19.06 ±3.67	>100
6		1	H	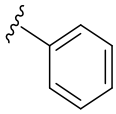	>100	14.38 ±1.11	10.3 ±0.8
8	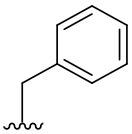	0	H	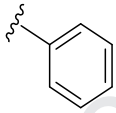	>100	6.55 ±0.79	>100
10	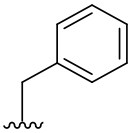	1	H	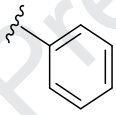	7.31 ±1.4	0.555 ±0.097	26.1 ±3.9
12		0	H	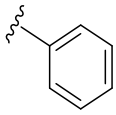	19.2 ±1.3	18.1 ±1.5	>100
14		1	H	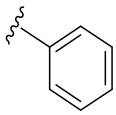	>100	1.433 ±0.306	>100
16		0	H	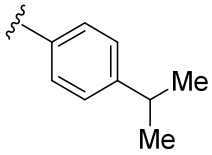	>100	>100	0.178 ±0.0093
18		1	H	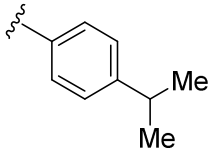	>100	24.3 ±0.3	0.316 ±0.0293
20	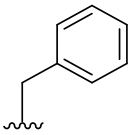	0	H	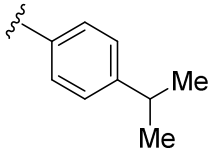	>100	1.74 ±0.55	>100

22	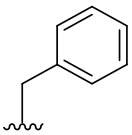	1	H	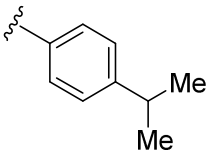	2.248 ±0.360	0.809 ±0.372	>100
24		0	H	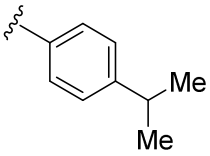	2.308 ±1.597	>100	>100
26		1	H	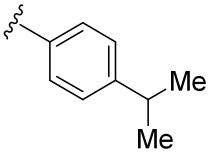	4.083 ±0.441	>100	>100
28		0	Me	Et	>100	11.4 ±2.6	>100
30		1	Me	Et	>100	>100	>100
32	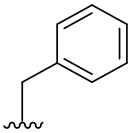	0	Me	Et	>100	>100	>100
34	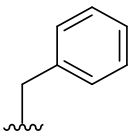	1	Me	Et	72.0 ±30.9	46.0 ±12.7	>100
36		0	Me	Et	>100	40.8 ±11.2	>100
38		1	Me	Et	>100	4.46 ±1.46	>100
Rasagiline[e]	/	/	/	/	>100	>100	0.036 ±0.004
Rivastigmine	/	/	/	/	19.8 ±2.6	1.439 ±0.228	>100

[a]**Compds** = compound number

[b]determined after 30 min preincubation of inhibitor with ChEs; data are expressed as mean ± SEM (n = 3)

[c]determined after 15 min preincubation of inhibitor with MAO-A/B; data are expressed as mean ± SEM (n = 3).

[d] = IC_{50} (hMAO-A) = 29.5 ±4.4 µM[c].

Table 3. Inhibitory potencies and structures of 1,3-disubstituted *N*-alkylpiperidine carbamates.

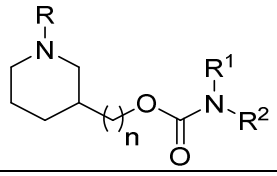

Compds[a]	R	n	R^1	R^2	hAChE[b] IC_{50} ±SEM (μM)	hBChE[b] IC_{50} ±SEM (μM)	hMAO-B[c] IC_{50} ±SEM (μM)
5		0	H	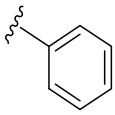	>100	84.5 ±19.8	>100
7		1	H	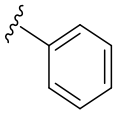	>100	29.6 ±4.7	>100
9	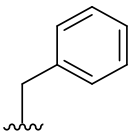	0	H	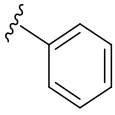	>100	0.46 ±0.049	33.3 ±7.5
11	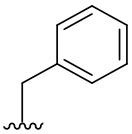	1	H	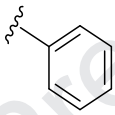	67.1 ±13.7	0.520 ±0.078	39.5 ±8.2
13		0	H	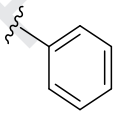	>100	0.0645 ±0.0115	>100
15		1	H	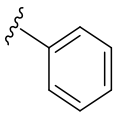	>100	0.1795 ±0.0233	>100
17		0	H	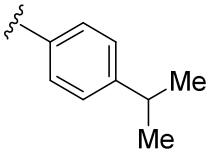	>100	>100	71.83 ±18.7
19		1	H	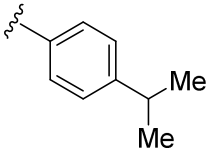	>100	17.75 ±3.7	2.857 ±0.267
21	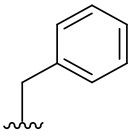	0	H	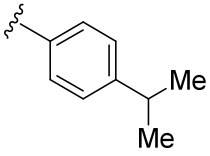	>100	3.25 ±0.94	29.3 ±3.4
23	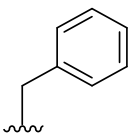	1	H	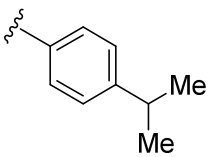	15.1 ±5.8	0.118 ±0.015	>100

25		0	H	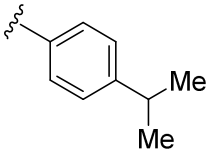	7.914 ±1.227	>100	>100
27		1	H	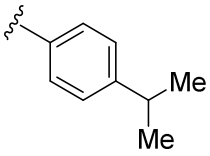	18.7 ±3.0	0.442 ±0.1752	>100
29		0	Me	Et	>100	>100	>100
31		1	Me	Et	>100	>100	>100
33	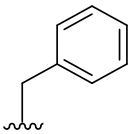	0	Me	Et	>100	21.0 ±6.8	>100
35	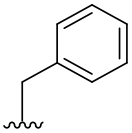	1	Me	Et	96.6 ±21.3	7.23 ±0.75	>100
37		0	Me	Et	>100	9.69 ±0.51	>100
39		1	Me	Et	>100	9.39 ±2.20	>100
Rasagiline[d]	/	/	/	/	>100	>100	0.036 ±0.004
Rivastigmine	/	/	/	/	19.8 ±2.6	1.439 ±0.228	>100

[a]**Compds** = compound number

[b]determined after 30 min preincubation of inhibitor with ChEs; data are expressed as mean ± SEM (n = 3)

[c]determined after 15 min preincubation of inhibitor with MAO-A/B; data are expressed as mean ± SEM (n = 3).

[d] = IC_{50} (hMAO-A) = 29.5 ±4.4 μM[c].

2.4. Structure–activity relationships

2.4.1. Structure–activity relationships of 1,4-disubstituted *N*-alkylpiperidine carbamates

Structure–activity relationships (SARs) of 1,4-disubstituted *N*-alkylpiperidine carbamates is presented in Figure 3. *N*-Benzylpiperidine **22** (IC_{50} = 2.25 µM) and *N*-(2,3-dihydro-1*H*-inden-2-yl)piperidine **24** (IC_{50} = 2.31 µM) are the most potent hAChE inhibitors in this series. The *i*Pr- group on the benzene ring of the carbamate group is needed for hAChE inhibition, as removing it from compounds **22** and **24** reduces the inhibitory potencies (**10**, IC_{50} = 7.31 µM; **12**, IC_{50} = 19.2 µM). *N*-Propargylpiperidines and (ethyl)methylcarbamates, with the exception of the very weak hAChE inhibitor **34** (IC_{50} = 72.0 µM), are inactive as hAChE inhibitors (IC_{50} > 100 µM).

N-Benzylpiperidine **10** (IC_{50} = 0.56 µM) is the most potent hBChE inhibitor of the series. Replacing the benzyl group with a 2,3-dihydro-1*H*-inden-2-yl group in **14** (IC_{50} = 1.43 µM) or a propargyl group in compound **6** (IC_{50} = 14.38 µM) reduces the inhibitory potencies by up to 25-fold. In contrast to hAChE inhibition, the presence of the *i*Pr- group on the benzene ring of the carbamate group reduces hBChE inhibitory potency. Carbamate **20** (IC_{50} = 1.74 µM) is the exception to this rule, since it is almost 4-fold more potent than the benzene counterpart **8** (IC_{50} = 6.55 µM). 1,4-Disubstituted *N*-alkylpiperidine carbamates with a methylene linker between the piperidine ring and the carbamate moiety (n = 1, Figure 3) are more potent hBChE inhibitors than compounds with the carbamate group bound directly to the piperidine ring (n = 0, Figure 3). Again, there is an exception to this rule: compound **28** (IC_{50} = 11.40 µM), which has an inactive "methylene" counterpart **30** (IC_{50} > 100 µM).

N-Propargylpiperidine **16** (IC_{50} = 0.18 µM) is the most potent hMAO-B inhibitor of this series. Inserting a methylene group between the piperidine ring and the carbamate moiety (n = 1, Figure 3) does not affect the inhibition to a significant extent (**18**, IC_{50} = 0.32 µM). Similar to hAChE inhibition, the *i*Pr- group on the benzene ring of the carbamate group is needed for hMAO-B inhibition. Removing this group from compound **18** reduces the

inhibitory potency by more than 30-fold (**6**; IC_{50} = 10.3 µM). *N*-Benzylpiperidine **10** (IC_{50} = 26.1 µM) is the only to inhibit hMAO-B inhibitor devoid of archetypal *N*-propargylpiperidine moiety. Nonetheless, the inhibition of hMAO-B is comparable to the propargyl counterpart **6** (IC_{50} = 10.3 µM). All *N*-(2,3-dihydro-1*H*-inden-2-yl)piperidines and (ethyl)methylcarbamates are inactive as hMAO-B inhibitors (IC_{50} > 100 µM).

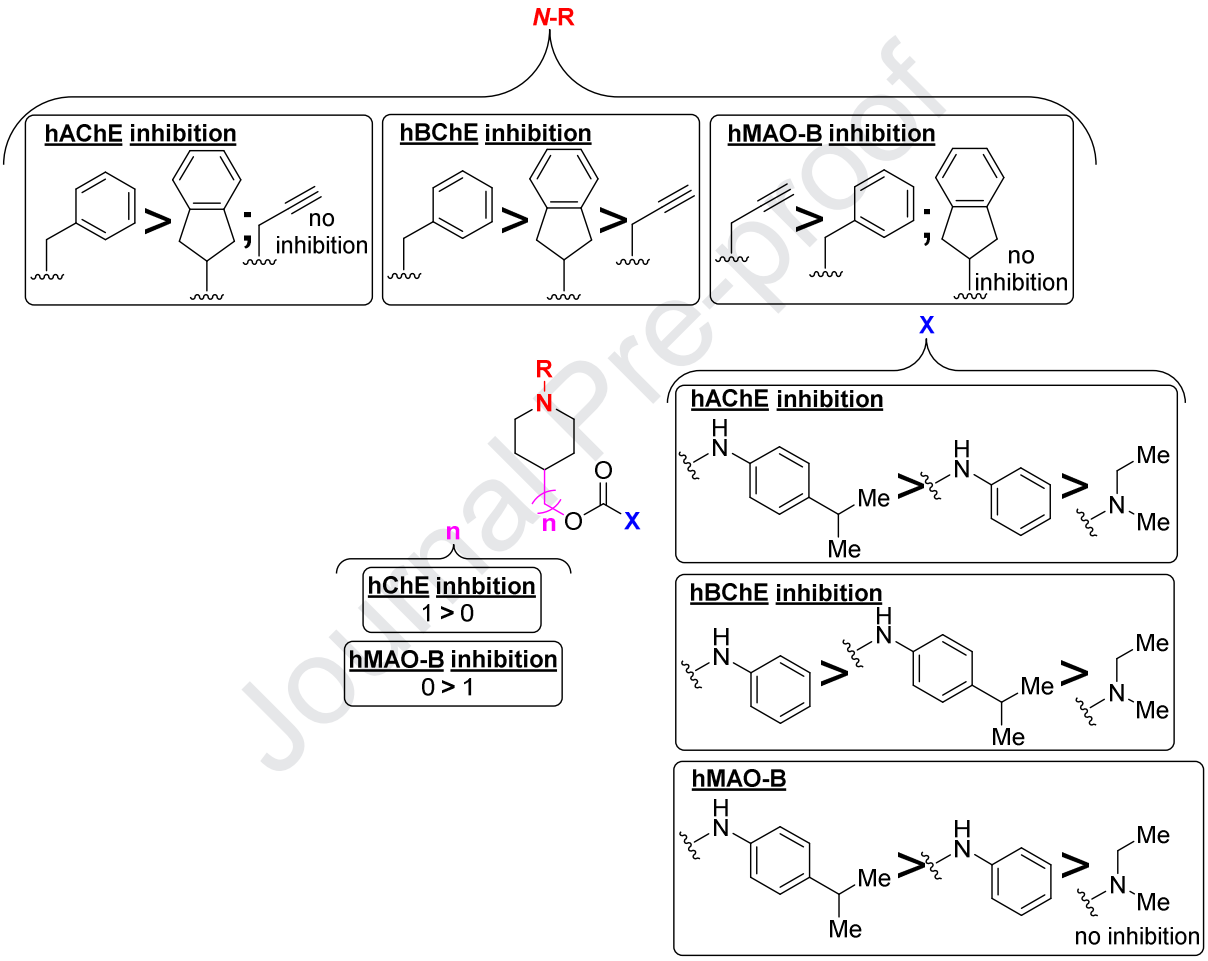

Figure 3. SARs of 1,4-disubstituted *N*-alkylpiperidine carbamates.

2.4.2 The structure–activity relationships of 1,3-disubstituted *N*-alkylpiperidine carbamates

Structure–activity relationships (SARs) of 1,3-disubstituted *N*-alkylpiperidine carbamates is presented in Figure 4. Compound **25** (IC_{50} = 7.91 µM) is the most potent

hAChE inhibitor of the series. Inserting a methylene group between the piperidine ring and the carbamate moiety (n = 1, Figure 4) slightly reduces the inhibitory potency (**27**, IC_{50} = 18.70 µM). Similar to 1,4-disubstituted piperidines, the *i*Pr- group on the benzene ring of the carbamate group is again needed for hAChE inhibition. Removing this group from compound **23** (IC_{50} = 15.10 µM) reduces the inhibitory potency (**11**, IC_{50} = 67.10 µM). As observed with 1,4-disubstituted piperidines, *N*-propargylpiperidines and (ethyl)methylcarbamates, with the exception of the very weak hAChE inhibitor **35** (IC_{50} = 96.6 µM), are inactive as hAChE inhibitors (IC_{50} > 100 µM).

N-(2,3-Dihydro-1*H*-inden-2-yl)piperidine **13** (IC_{50} = 0.06 µM) is the most potent hBChE inhibitor of this series. Inserting a methylene group between the piperidine ring and the carbamate moiety (n = 1, Figure 4) increases the inhibitory potency of all 1,3-disubstituted *N*-alkylpiperidine carbamates, except compound **15** (IC_{50} = 0.18 µM), which is less potent than its "non-methylene" counterpart **13** (IC_{50} = 0.06 µM). As observed with 1,4-disubstituted piperidines, the presence of the *i*Pr- group on the benzene ring of the carbamate group reduces hBChE inhibitory potency. Carbamate **23** (IC_{50} = 0.12 µM) is the exception to this rule, since it is almost four-fold more potent than its benzene counterpart **11** (IC_{50} = 0.52 µM). *N*-Propargylpiperidines and (ethyl)methylcarbamates are practically inactive as hBChE inhibitors.

N-Propargylpiperidine **19** (IC_{50} = 2.86 µM) is the most potent hMAO-B inhibitor of this series. Removing the methylene group between the piperidine ring and the carbamate moiety (n = 0, Figure 4) reduces the inhibitory potency significantly (**17**, IC_{50} = 71.83 µM). Replacing the propargyl group of compound **19** with a benzyl group (**21**, IC_{50} = 29.30 µM) has a similar effect: the inhibitory potency is reduced by more than tenfold. Similarly as with 1,4-disubstituted piperidines, all *N*-(2,3-dihydro-1*H*-inden-2-yl)piperidines and (ethyl)methylcarbamates are inactive as hMAO-B inhibitors (IC_{50} > 100 µM).

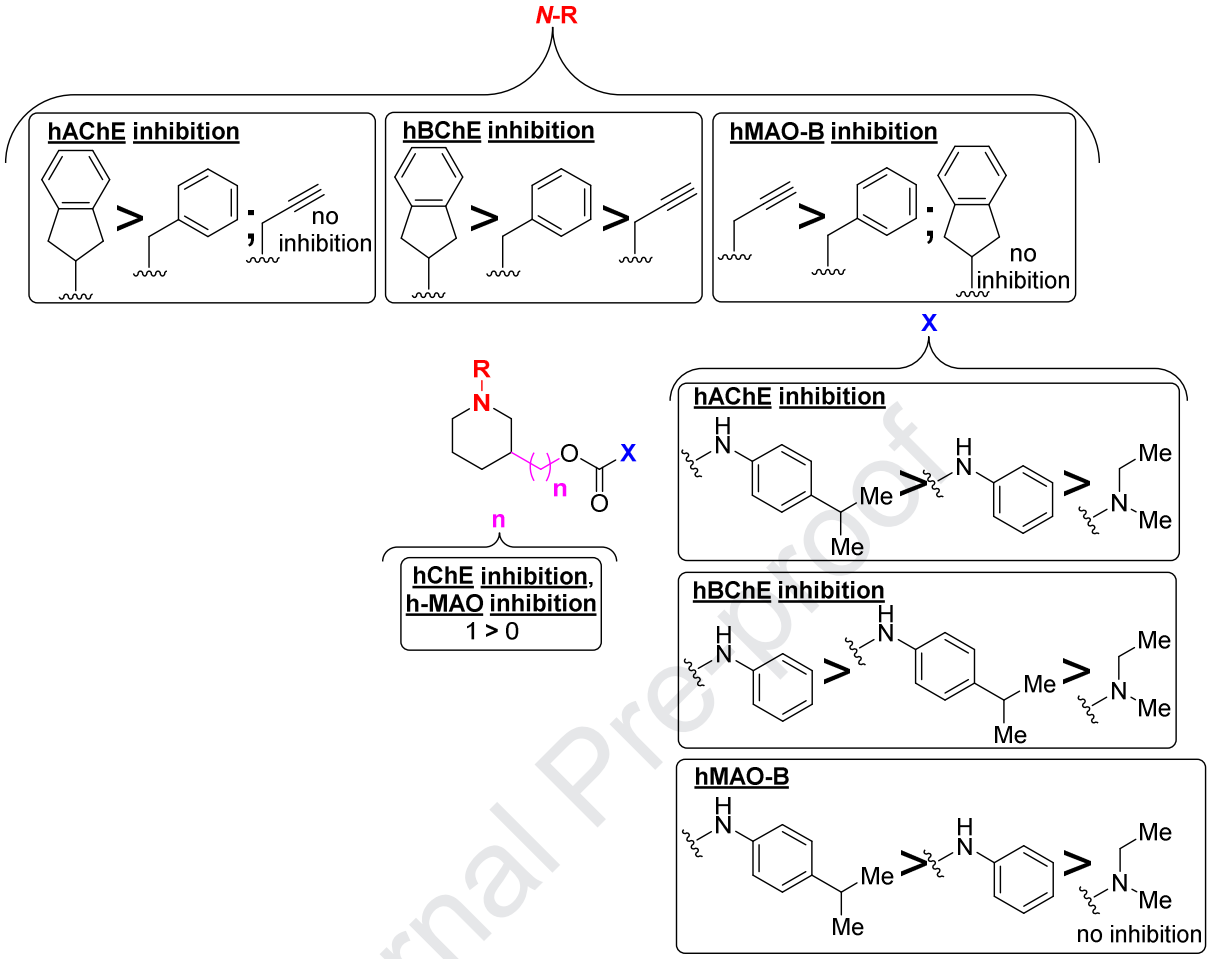

Figure 4. SARs of 1,3-disubstituted *N*-alkylpiperidine carbamates.

2.5. Mechanism of hChE and hMAO-B inhibition

To determine the mechanism of inhibition, reversibility 100-fold dilution assay and IC_{50} curve shift assays[34] were performed with hAChE, hBChE and hMAO-B inhibitor **10**, the most potent selective hBChE inhibitor **13**, the most potent selective hMAO-B inhibitor **16**, and dual hAChE and hBChE inhibitor **22**.

In the 100-dilution assay, irreversible inhibitors maintain inhibition after dilution of the preincubated mixture (Figure 5). In the IC_{50} curve shift assay, IC_{50} values of time-dependent inhibitors decrease with prolongation of incubation time (Figures 6 and 7). Results of these assays show that compounds **10**, **13**, and **22** are reversible (Figure 5A and 5B) and

non-time-dependent inhibitors (Figure 6) of hAChE and/or hBChE. The results also show that compound **16** is an irreversible (Figure 5D) and time-dependent inhibitor (Figure 7) of hMAO-B, while compound **10** is not (Figures 5D and 7). This was expected since compound **16** is an *N*-propargylamine and compound **10** is a *N*-benzylpiperidine derivative, not capable of forming a covalent bond with hMAO-B.

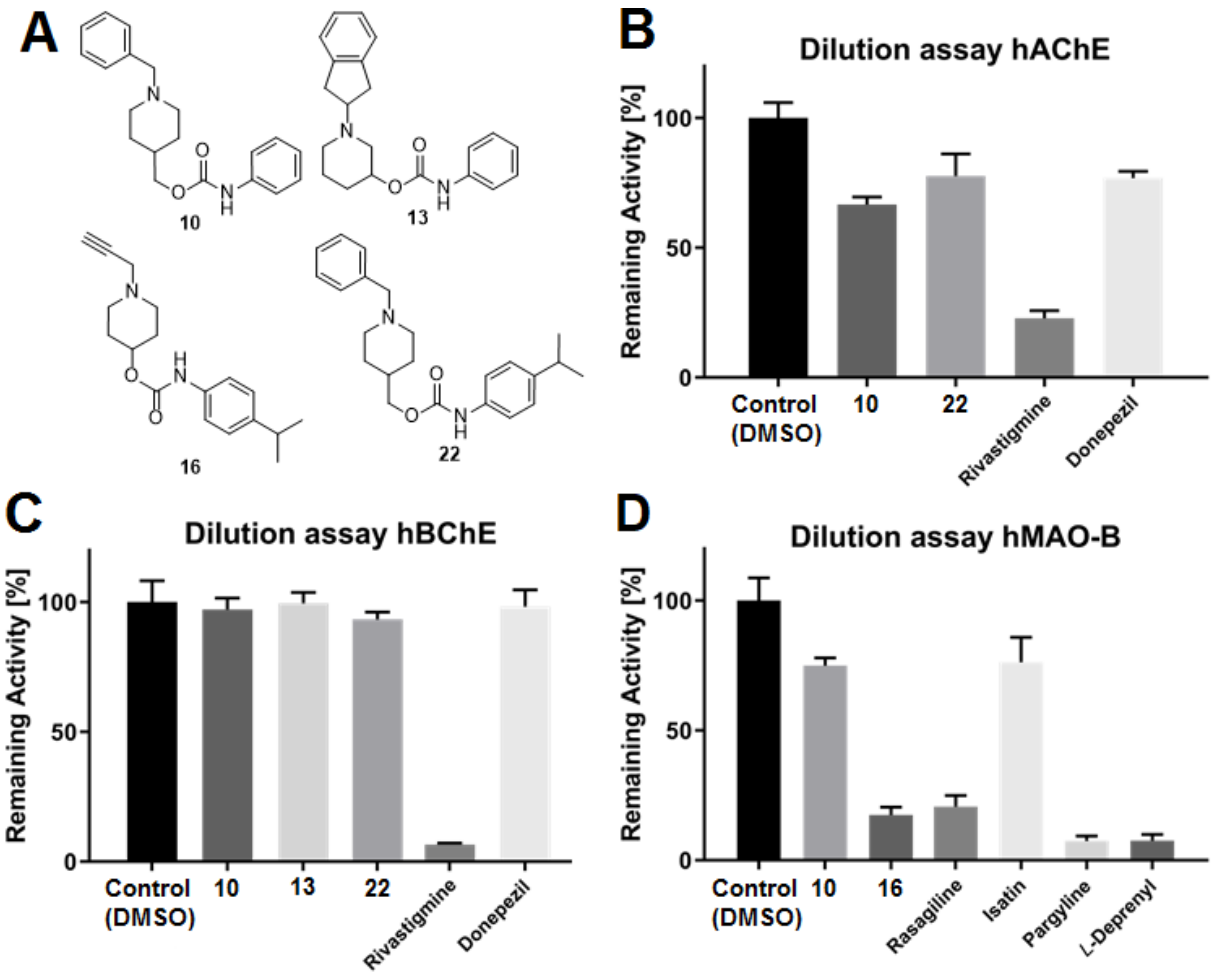

Figure 5. Dilution assay. Structures of compounds **10**, **13**, **16**, and **22** (A). Recovery of hAChE (B), hBChE (C), and hMAO-B (D) activity after 100-fold dilution following 15 min incubation for hMAO-B (30 min for ChEs) at 37 °C (at room temperature for ChEs) of the 100× enzyme concentration with 10-fold the IC_{50} of compounds **10**, **13**, **16**, **22**, rivastigmine (irreversible hChE inhibitor), donepezil (reversible hAChE inhibitor), rasagiline, paragyline, *L*-deprenyl (irreversible hMAO-B inhibitors) and isatin (reversible hMAO-B inhibitor). The control (DMSO) was carried out in the absence of inhibitor

and diluted in the same way. Data are expressed as percentages of control ± SEM of three independent experiments (each performed in quadruplicate).

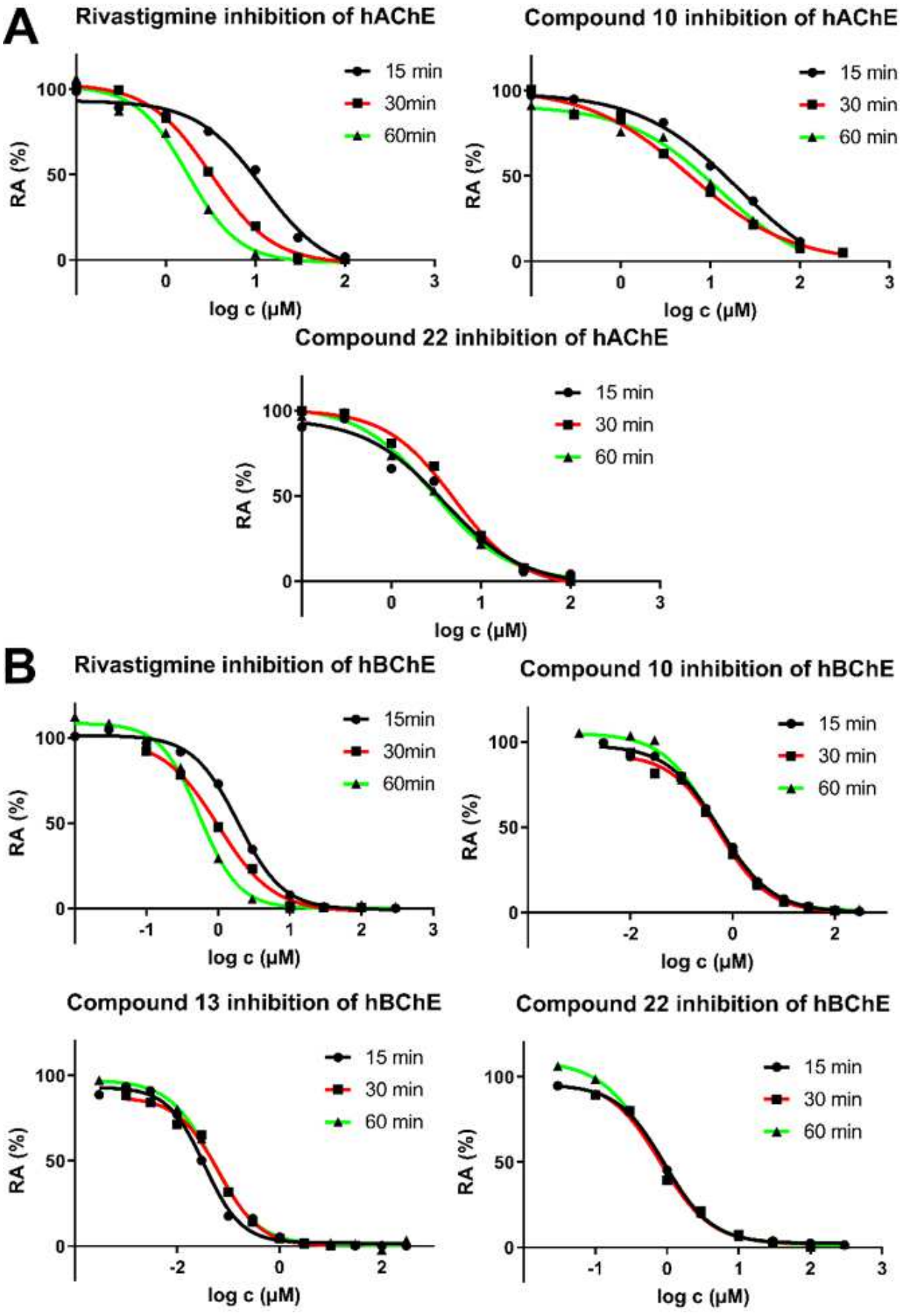
A
Rivastigmine inhibition of hAChE
15 min
30min
60min
RA (%)
log c (μM)
Compound 10 inhibition of hAChE
15 min
30 min
60 min
RA (%)
log c (μM)
Compound 22 inhibition of hAChE
15 min
30 min
60 min
RA (%)
log c (μM)
B
Rivastigmine inhibition of hBChE
15min
30min
60min
RA (%)
log c (μM)
Compound 10 inhibition of hBChE
15 min
30 min
60 min
RA (%)
log c (μM)
Compound 13 inhibition of hBChE
15 min
30 min
60 min
RA (%)
log c (μM)
Compound 22 inhibition of hBChE
15 min
30 min
60 min
RA (%)
log c (μM)

Figure 6. IC_{50} curve shift assay for hChE inhibition. Inhibiton of hAChE (A) and hBChE (B) by rivastigmine (positive control for time-dependent hChE inhibition) and compounds **10**, **13**, and **22** at various pre-incubation times (indicated in the legends). For inhibition of hBChE by compound **13** at additional pre-incubation times (1, 5, 15, 30, and 60 min) see Supporting Figure S1. RA = residual activity.

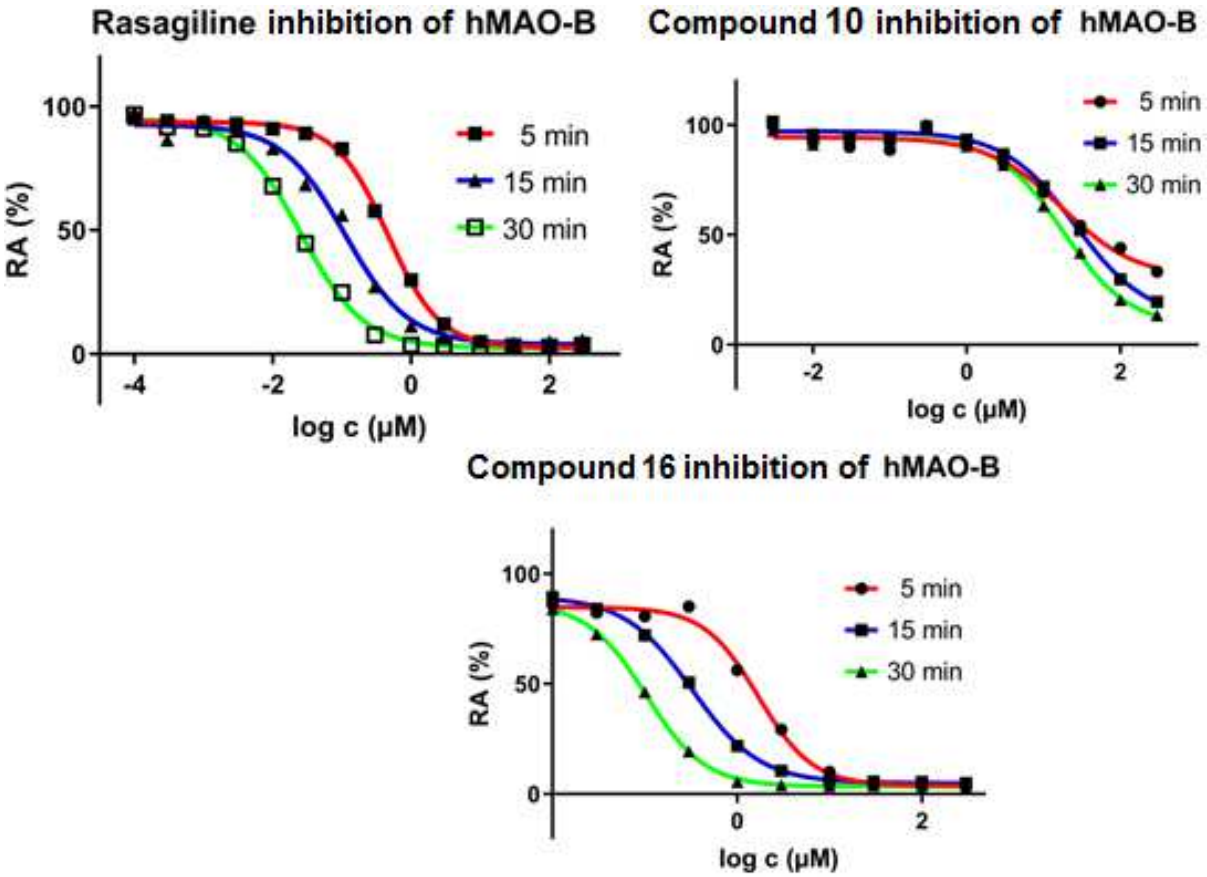

Figure 7. IC_{50} curve shift assay for hMAO-B inhibition. Inhibiton of hMAO-B by rasagiline (positive control for time-dependent hMAO-B inhibition) and compounds **10** and **16** at various pre-incubation times (indicated in the legends). RA = residual activity.

2.6. Co-crystal structure of hBChE in complex with compound 13

The crystal structure of compound **13** bound to hBChE was resolved at 2.5 Å resolution (Supporting Table S1). The crystals were obtained by the hanging drop method, then soaked with compound **13** at 1 mM final ligand concentration (1% DMSO). Close

examination of the binding mode explains why compound **13,** in particular, does not inhibit hBChE in a covalent manner. The phenyl substituent occupies the acyl-binding pocket of hBChE, which is defined by residues Trp231, Leu286, Val288 and Phe398, and forms a T-stacking interaction (i.e., π-stacking) with Trp231 (Figure 8A). It is important to compare the binding poses of compounds **13** and **1** because compound **13** is a new lead compound derived from hit compound **1**. Importantly, despite the 2D similarity of compounds **1** and **13** (Figure 8C), this does not necessarily lead to comparable binding poses. Thus, special attention should always be placed to the structural elucidation or molecular modelling studies, which can reveal the reasons for the deviations in the modes of inhibition. Contrary to the hit inhibitor [IC_{50}(hBChE) = 21.3 nM][27], the piperidine ring of carbamate **13** is flipped with the indene moiety pointing towards Trp82 in the choline-binding pocket (Figure 8B). The piperidine nitrogen occupies exactly the same position as in the parent inhibitor, and forms a π-cation interaction with Tyr332, which is a pivotal interaction for the inhibition of hBChE. Additionally, compound **13** is stabilized by H-bonds between the carbamate nitrogen and oxygen with two water molecules. The latter are also H-bonded to the backbone carbonyl groups of Pro285 and Ser287, and the piperidine nitrogen. The stabilization of the carbamate core with several H-bonds places the inhibitor in the middle of the active site gorge with the carbamate carbonyl group at the distance of 6.6 Å from Ser198, which precludes the covalent binding of compound **13**. This pose and inhibition data clearly demonstrate that introduction of a carbamate group into a compound does not necessarily produce a pseudo-irreversible ChE inhibitor.

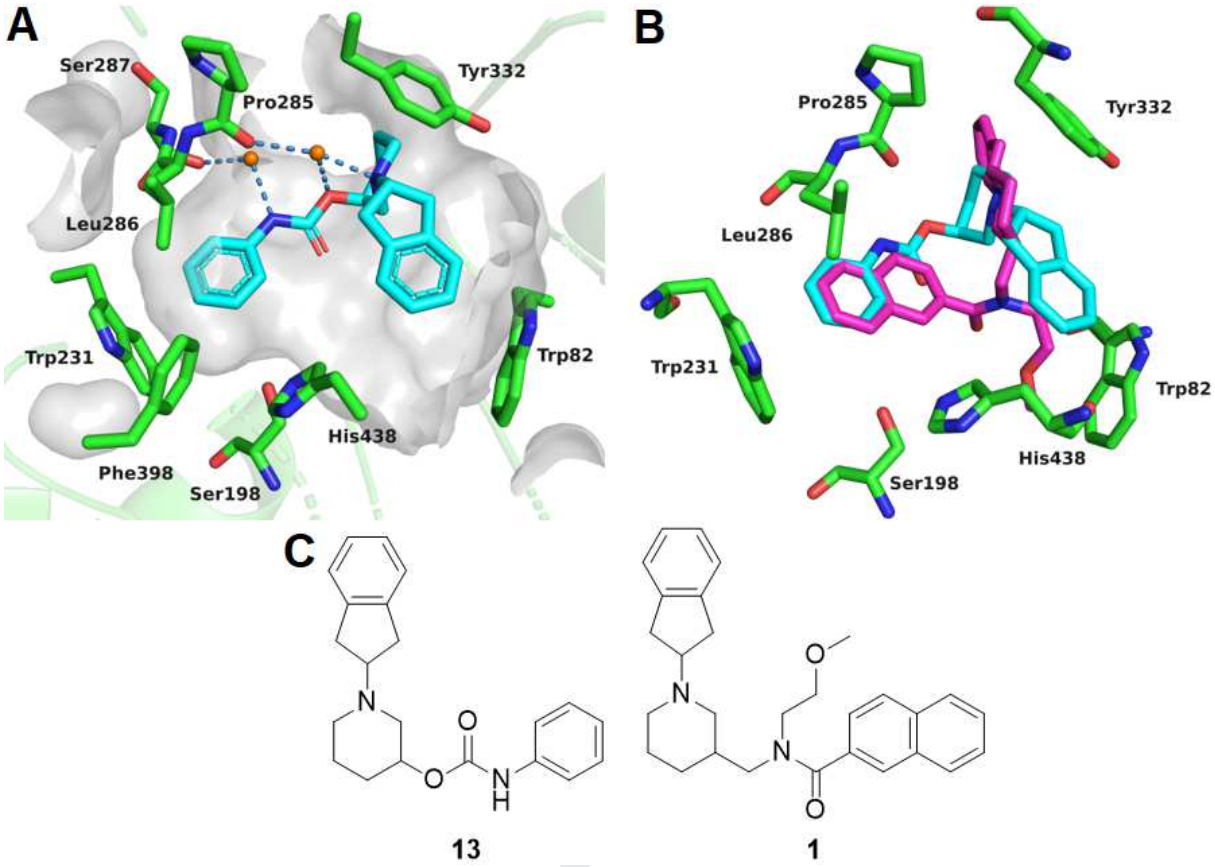

Figure 8. Crystal structure of hBChE in complex with compound 13 (PDB 6SAM; resolution 2.5 Å). (A) Compound **13** (cyan) and the key residues of hBChE (green) involved in the binding are shown as sticks. Water molecules are presented as orange spheres and hydrogen bonds are blue dotted lines. (B) Alignment of the crystal structures of compound **13** (cyan) and the parent hit compound **1** (magenta) in the active site of hBChE. (C) Structures of compounds **13** and **1**.

2.7. Inhibition of $A\beta_{1-42}$ aggregation

The inhibitory activity of carbamates **10**, **13**, **16**, and **22** against $A\beta_{1-42}$ aggregation was evaluated with the thioflavine-T (ThT) fluorometric assay[40]. Compound **16** showed modest $A\beta_{1-42}$ anti-aggregation effects, with 25.7% inhibition of $A\beta_{1-42}$ aggregation (Table 4).

Table 4. Inhibition of $A\beta_{1-42}$ aggregation by *N*-alkylpiperidine carbamates 10, 13, 16, 22, rivastigmine, rasagiline, resveratrol and donepezil.

Compound	Inhibition of $A\beta_{1-42}$ aggregation[a]

10	n.i.[b]
13	n.i.[b]
16	25.7 ± 0.8%*
22	n.i.[b]
Rivastigmine tartrate	n.i.[b]
Rasagiline mesylate	n.i.[b]
Resveratrol	86.6 ± 11.6%*
Donepezil	n.i.[b]

[a] Percent inhibition at 10 μM compound and 1.5 μM $A\beta_{1-42}$. Percentage of inhibition means ± SD of three independent experiments (each performed in quadruplicate); [b] No inhibition (percent inhibition lower than 20%). Statistical analysis: one-way ANOVA, followed by *post-hoc* Bonferroni *t*-test (SigmaPlot v 12.0), compared to control experiment ($A\beta_{1-42}$ + DMSO); *$p < 0.05$.

2.8. *In vitro* blood-brain barrier permeation

As AD is a brain disease, drugs used for its treatment must partition into the brain by crossing the blood-brain barrier (BBB). Therefore, the brain permeation of compounds **10**, **13**, **16** and **22** was evaluated using the parallel artificial membrane permeation assay (PAMPA)–BBB method, which is a high-throughput and low-cost assay used to exclude poorly permeable compounds from further testing (e.g., *in-vitro* assays on cell lines and *in-vivo* assays)[41]. Table 5 shows the negative logarithms of the effective permeabilities ($-\log P_e$) of *N*-alkylpiperidine carbamates **10**, **13**, **16,** and **22** and five reference drugs with known central nervous system penetration. For all of the *N*-alkylpiperidine carbamates, the $-\log P_e$ values are lower than the limit for high permeability (5.6), which suggests that these compounds should be able to cross BBB.

Table 5. *In-vitro* BBB permeation of carbamates and reference drugs.

Compounds	**PAMPA-BBB**	
	$-\log P_e$ (cm/s) mean ± SD	Permeabilty prediction[a]

10	5.31 ± 0.19	high
13	5.36 ± 0.04	high
16	5.01 ± 0.22	high
22	4.84 ± 0.21	high
Propranolol	5.11 ± 0.04	high
Lidocaine	4.79 ± 0.03	high
Verapamil	5.17 ± 0.03	high
Quinidine	5.12 ± 0.05	high
Theophylline	6.40 ± 0.05	low

[a] –logPe < 5.6, high permeability; –log*Pe* > 6.2, low permeability; intermediate –log*Pe* values (5.6 – 6.2) were labeled as intermediate BBB permeability.

2.9. Cytotoxicity and neuroprotective effects of compound 10, 13, 16 and 22

To determine whether *N*-alkylpiperidine carbamates share the non-cytotoxic and neuroprotective properties of the parent compounds **1**[27], **2**[28], and **3**[29], inhibitors **10**, **13**, **16** and **22** were characterized accordingly.

First, their cytotoxicity profiles were determined using the MTS **(**3-(4,5-dimethylthiazol-2-yl)-5-(3-carboxymethoxyphenyl)-2-(4-sulfophenyl)-2*H*-tetrazolium, inner salt) assay. Results show that all four compounds (**10**, **13**, **16** and **22**) were non-cytotoxic at 20 µM on SH-SY5Y cells (Figure 9A) and at 50 µM on HepG2 cells (Figure 9B).

We then determined whether compounds **10**, **13**, **16** and **22** can protect neuronal-like cells from toxic Aβ-species. Therefore, we examined neuronal death induced by 5 µM $A\beta_{1-42}$ in the absence and presence of 20 µM compounds **10**, **13**, **16** and **22**. In this assay, compounds that decrease the percentage of 7-aminoactinomycin D (7-AAD) positive cells have a neuroprotective effect against $A\beta_{1-42}$-induced toxicity. Treatment of SH-SY5Y cells with 5 µM of $A\beta_{1-42}$ caused significant toxicity, as evident from the significant increase of 7-AAD positive cells (Figure 9C), whereas hMAO-B inhibitors **10** and **16** diminished $A\beta_{1-42}$-induced cell death (Figure 9C). The neuroprotective effect of compound **10** is independent of $A\beta_{1-42}$ aggregation, as, compounds **10** at 10 µM did not inhibit $A\beta_{1-42}$ aggregation in the ThT

fluorometric assay (Table 4). On the other hand, the neuroprotective effect of compound **16** could be the result of its $A\beta_{1–42}$ anti-aggregation effects (Table 4).

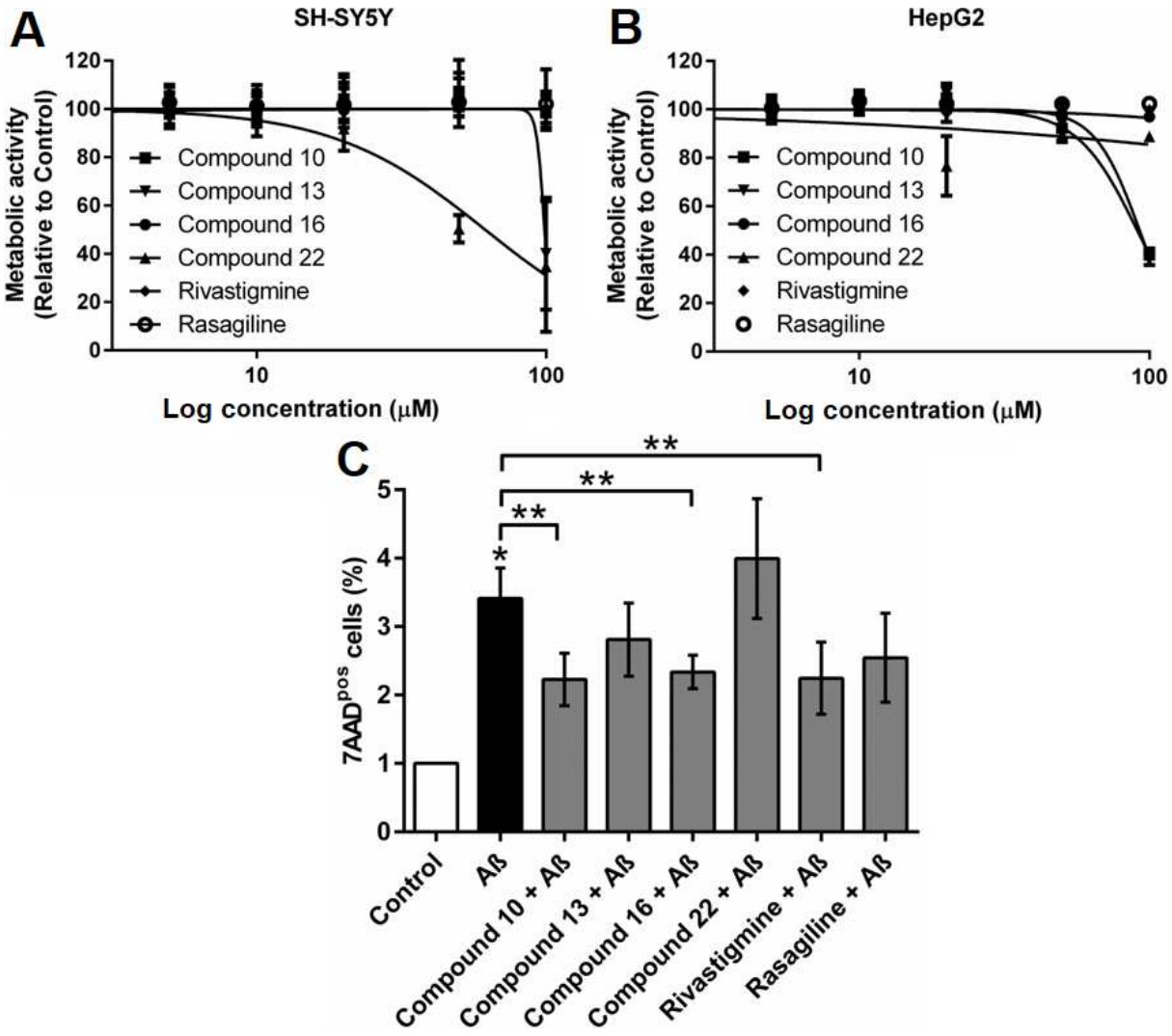

Figure 9. Cytotoxicity and neuroprotective effects of compound 10, 13, 16 and 22. Cytotoxicity in SH-SY5Y (A) and HepG2 cells (B). Cells were incubated in the presence of increasing concentrations of compounds (1–100 μM) in reduced-serum medium. After 48 h, the cell viability was evaluated using the MTS assay. The control group (DMSO) was considered as 100% cell viability. Data are means ± SD of three independent experiments, each carried out in quadruplicate. (C) The effect on $A\beta_{1-42}$-induced toxicity in SH-SY5Y cells. Cells were treated with $A\beta_{1-42}$ (5 μM) in the absence or presence of compounds (20 μM) in reduced-serum medium. After 48 h treatment, neuroprotective effect was evaluated by flow cytometry analysis of 7AAD staining. The graph shows the results of

quantitative analysis and indicates the percentage of dead cells, a fraction of 7AAD positive cells ($7AAD^{pos}$). Results are means ± SD of at least two independent assays, each carried out in duplicate. *P < 0.05, **P < 0.1

It has been shown recently that $A\beta_{1-42}$ aggregation initiates the cellular uptake of Aβ oligomers and fibrils and subsequently the cytotoxicity[42]. Therefore, the next step was to evaluate the effects of neuroprotective compounds **10** and **16** on the distribution of $A\beta_{1-42}$ in SH-SY5Y cells. For this experiment, cells were stained for amyloid fibrils after the treatment with monomeric $A\beta_{1-42}$ peptide in the absence or presence of compounds **10** and **16**. Staining with the amyloid precursor protein (APP)/Aβ antibody revealed large extent of the Aβ aggregates present in $A\beta_{1-42}$ peptide-treated SH-SY5Y cells, whereas no such staining was observed in non-treated (Control) cells as seen in Figure 10. Moreover, no noticeable difference in the distribution of the amyloid fibrils in the $A\beta_{1-42}$ peptide-treated SH-SY5Y cells was observed in the presence of the compound **10**, whereas less Aβ aggregates were observed in the treated cells in the presence of compound **16** (Figure 10). This is in agreement with the results of compound **10** and **16** obtained in the ThT fluorometric assay (Table 2).

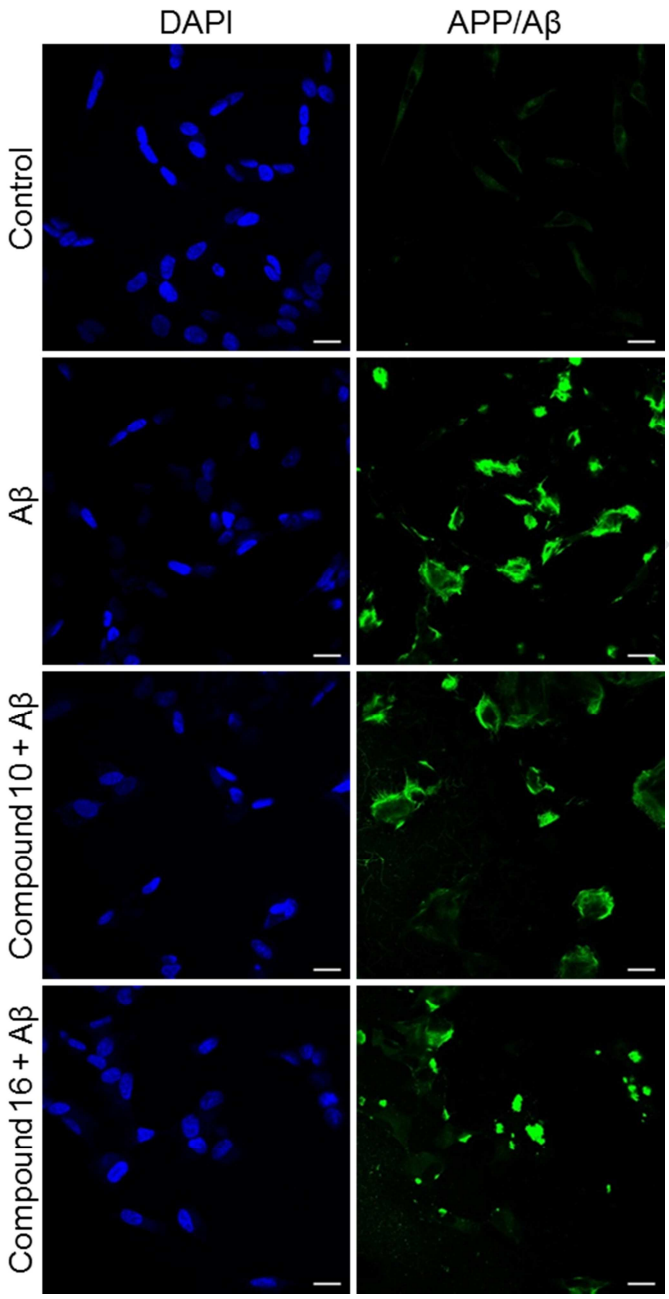

Figure 10. The effect of compounds 10 and 16 on the distribution of $A\beta_{1-42}$ in SH-SY5Y cells. Cells were treated with $A\beta_{1-42}$ (5 µM) in the absence or presence of the compound **10** (20 µM) or compound **16** (20 µM) in reduced-serum medium. After 48 h treatment, SH-SY5Y cells were stained for APP/Aβ with 4′,6-diamidino-2-phenylindole (DAPI) counterstained nuclei and then visualized with confocal microscope Carl Zeiss LSM 710 and 63× oil immersion objective. Images were edited by using ZEN2011 software. Scale bar, 20 µm.

2.10. Stability of the synthesized carbamates

In general, carbamates are chemically and enzymatically more stable than the corresponding esters, but more susceptible to hydrolysis than corresponding amides. The bioconversion of carbamates requires esterases which, upon hydrolysis, release the parent phenol or alcohol and unstable carbamic acid. The latter breaks down to the corresponding amine and carbon dioxide (Scheme 1). Carbamates derived from alcohols show higher chemical stability than those from phenols due to the lower pKa of phenols in comparison to alcohols[43].

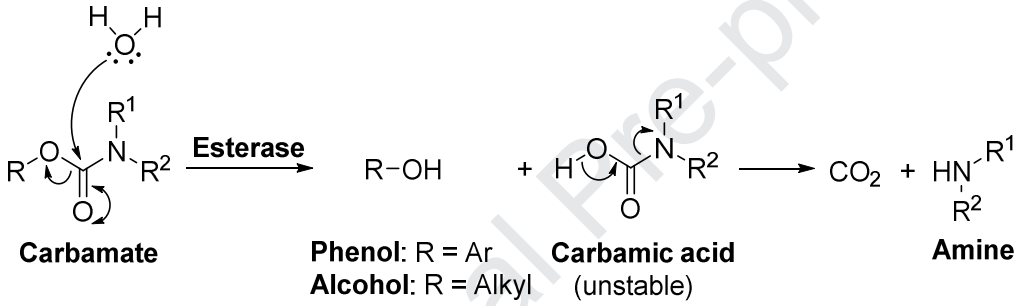

Scheme 1. Bioconversion of carbamates.

Therefore, we expect our carbamates to be biologically stable because they are chemically stabile under the synthetic and isolation conditions described in the **Methods** setion, they don't react covalently with two esterases (AChE and BChE), and are all derived from alcohols and not from phenols as are rivastigmine, (–)-phenserine and bisnorcymserine (Figure 2).

3. Conclusions

We present the design, synthesis, and biochemical evaluation of 36 *N*-alkylpiperidine carbamates as potential multifunctional ligands for AD. The most promising compounds of the series are compounds **10** [inhibition of hAChE (IC_{50} = 7.31 μM), hBChE (IC_{50} = 0.555

μM) and hMAO-B (IC_{50} = 7.31 μM)], **13** [selective inhibition of hBChE (IC_{50} = 0.0645 μM)], **16** [selective hMAO-B inhibition (IC_{50} = 0.178 μM) and **22** [inhibition of hAChE (IC_{50} = 2.248 μM) and hBChE (IC_{50} = 0.809 μM)]. Kinetic experiments were used to determine their mechanism of hChE and hMAO-B inhibition. Compounds **10**, **13**, and **22** are reversible and non-time-dependent inhibitors of hAChE and/ or hBChE. These experiments also show that compound **16** is an irreversible and time-dependent inhibitor of hMAO-B, while compound **10** is not. The crystal structure of compound **13** in complex with hBChE revealed its mode of binding, confirmed the non-covalent mechanism of inhibition, and opened the possibility for further optimization of *N*-alkylpiperidine carbamates. The results from the PAMPA-BBB assay indicate that compounds **10**, **13**, **16** and **22** should all cross the BBB. These compounds are noncytotoxic; moreover, compounds **10** and **16** also prevented $A\beta_{1-42}$-induced neuronal cell death. The neuroprotective effects of compound **16** may be the result of its $A\beta_{1-42}$ anti-aggregation effects. *N*-alkylpiperidine carbamates reported herein confirmed our hypothesis that novel anti-AD compounds, capable of interacting with one or more targets in AD pathogenesis, can be developed by combining moieties of known anti-AD compounds.

4. Methods

4.1. General chemistry methods

^{1}H-NMR and ^{13}C-NMR were recorded at 400.130 MHz and 100.613 MHz, respectively, on an NMR spectrophotometer (Bruker Avance III). The chemical shifts (δ) are reported in parts per million (ppm) and are referenced to the deuterated solvent used. The coupling constants (*J*) are reported in Hz, and the splitting patterns are indicated as: s, singlet; bs, broad singlet; d, doublet; dd, doublet of doublets; td, triplet of doublets; h, hextet; m, multiplet; t, triplet; bt, broad triplet; dt, doublet of triplets; tt, triplet of triplets; q, quartet; qd, quartet of doublets. Infrared (IR) spectra were recorded on a FT-IR spectrometer (System

Spectrum BX; Perkin-Elmer). ATR IR spectra were recorded on a FT-IR spectrometer (Thermo Nicolet Nexus 470 ESP). Mass spectra were recorded on a LC-MS/MS system (Q Executive Plus; Thermo Scientific, MA, USA). Evaporation of the solvents was performed under reduced pressure. Reagents and solvents were purchased from Acros Organics, Alfa Aesar, Euriso-Top, Fluka, Merck, Sigma-Aldrich, and TCI Europe, and were used without further purification, unless otherwise stated. Flash column chromatography was performed on silica gel 60 for column chromatography (particle size, 230–400 mesh). Analytical thin-layer chromatography was performed on silica gel aluminium sheets (0.20 mm; 60 F254; Merck), with visualization using ultraviolet light and/or visualization reagents. Analytical reversed-phase UPLC method A was performed on an LC system (Dionex Ultimate 3000 Binary Rapid Separation; Thermo Scientific) equipped with an autosampler, a binary pump system, a photodiode array detector, a thermostated column compartment, and the Chromeleon Chromatography Data System. The detector on UPLC system was set to 210 nm and 254 nm. The column used for method A and was a C18 analytical column (50 × 2.1 mm, 1.8 µm; Acquity UPLC HSS C18SB). The column was thermostated at 40 °C.

***Method A*:** The sample solution (2 µL; 0.2 mg/mL in MeCN) was injected and eluted at a flow rate of 0.4 mL/min, using a linear gradient of mobile phase A (MeCN) and mobile phase B (0.1% [v/v] aqueous TFA). The gradient for method A (for mobile phase A) was: 0–5 min, 10%–90%; 5–7.5 min, 90%; 7.5–8 min, 90–10%.

4.2. General synthetic procedures

4.2.1. General procedure for synthesis of carbamate with isocyanate (general procedure 1)

The alcohol (1.0 equiv.) was dissolved in CH_2Cl_2 at room temperature. The solution was stirred, and isocyanate (1.2 equiv.) was added, followed by 4-DMAP (0.1 equiv.). After 24 h, the solvent was evaporated and the crude product was purified by flash column chromatography.

4.2.2. General procedure for synthesis of ethyl(methyl)carbamate with *N*-ethyl-*N*-methylcarbamoyl chloride (general procedure 2)

The alcohol (1.0 equiv.) was dissolved in pyridine at room temperature. The solution was stirred and *N*-ethyl-*N*-methylcarbamoyl chloride (1.2 equiv.) was added. The reaction mixture was stirred under argon at reflux (120 °C) for 24 h. The mixture was cooled to room and the solvent was evaporated. The crude product was purified by flash column chromatography.

4.3. Characterization of the synthesized compounds

Synthesis of 1-(prop-2-yn-1-yl)piperidin-4-yl phenylcarbamate (4)

Synthesized from 1-(prop-2-yn-1-yl)piperidin-4-ol (**44**) (0.210 g, 1.509 mmol, 1.0 equiv.), phenyl isocyanate (0.197 mL, 1.811 mmol, 1.2 equiv.) and 4-DMAP (0.018 g, 0.151 mmol, 0.1 equiv.) in CH_2Cl_2 (5 mL) via general procedure 1. The crude product was purified by flash column chromatography using EtOAc/*n*-hexane (2:1, v/v) as the eluent, to produce 0.331 g of **4** as a colourless oil which solidified into a white solid after cooling (85% yield). R_f = 0.23 (EtOAc/*n*-hexane, 2:1, v/v). IR (ATR): 3283, 2961, 2810, 1712, 1546, 1310, 1231, 1057, 1028, 739, 677, 648 cm^{-1}. ^{1}H-NMR ($CDCl_3$): δ 1.75–1.84 (m, 2H), 1.99–2.05 (m, 2H), 2.27 (t, *J* = 2.4 Hz, 1H), 2.44–2.50 (m, 2H), 2.77–2.82 (m, 2H), 3.32 (d, *J* = 2.5 Hz, 2H), 4.77–4.83 (m, 1H), 6.64 (bs, 1H), 7.04–7.08 (m, 1H), 7.28–7.33 (m, 2H), 7.38 (bd, *J* = 8.0 Hz, 2H). ^{13}C-NMR ($CDCl_3$): δ 30.85, 46.70, 49.47, 70.39, 73.19, 78.61, 118.57, 123.17, 128.84, 137.86,

152.92. HRMS (ESI+): *m/z* calcd for $C_{15}H_{19}O_2N_2$ 259.1441; found 259.1436. UPLC purity, 99% at 254 nm (method A , t_R = 2.070 min).

Synthesis of 1-(prop-2-yn-1-yl)piperidin-3-yl phenylcarbamate (5)

Synthesized from 1-(prop-2-yn-1-yl)piperidin-3-ol (**45**) (0.220 g, 1.580 mmol, 1.0 equiv.), phenyl isocyanate (0.197 mL, 1.811 mmol, 1.2 equiv.) and 4-DMAP (0.021 g, 0.158 mmol, 0.1 equiv.) in CH_2Cl_2 (5 mL) via general procedure 1. The crude product was purified by flash column chromatography using EtOAc/*n*-hexane (2:3, v/v) as the eluent, to produce 0.355 g of **5** as a colourless oil which solidified into a white solid after cooling (87% yield). R_f = 0.50 (EtOAc/*n*-hexane, 2:1, v/v). IR (ATR): 3298, 2949, 1693, 1546, 1442, 1234, 1054, 907, 759, 743, 698, 509 cm^{-1}. ^{1}H-NMR ($CDCl_3$): δ 1.60–1.71 (m, 2H), 1.76–1.81 (m, 1H), 1.83–1.93 (m, 1H), 2.26 (t, *J* = 2.4 Hz, 1H), 2.50–2.60 (m, 2H), 2.64–2.68 (m, 1H), 2.77–2.80 (m, 1H), 3.38 (d, *J* = 2.4 Hz, 2H), 4.96–5.01 (m, 1H), 6.76 (bs, 1H), 7.03–7.07 (m, 1H), 7.27–7.32 (m, 2H), 7.37 (d, *J* = 7.7 Hz, 2H). ^{13}C-NMR ($CDCl_3$): δ 21.82, 28.47, 46.86, 51.58, 55.53, 69.75, 73.54, 78.03, 118.39, 123.11, 128.84, 137.85, 152.79. HRMS (ESI+): *m/z* calcd for $C_{15}H_{19}O_2N_2$ 259.1441; found 259.1438. UPLC purity, 97% at 254 nm (method A, t_R = 2.083 min).

Synthesis of (1-(prop-2-yn-1-yl)piperidin-4-yl)methyl phenylcarbamate (6)

Synthesized from (1-(prop-2-yn-1-yl)piperidin-4-yl)methanol (**46**) (0.220 g, 1.436 mmol, 1.0 equiv.), phenyl isocyanate (0.187 mL, 1.723 mmol, 1.2 equiv.) and 4-DMAP (0.018 g, 0.144 mmol, 0.1 equiv.) in CH_2Cl_2 (5 mL) via general procedure 1. The crude product was purified by flash column chromatography using EtOAc/*n*-hexane (2:1, v/v) as the eluent, to produce 0.358 g of **6** as a colourless oil which solidified into a white solid after cooling (90% yield). R_f = 0.20 (EtOAc/*n*-hexane, 2:1, v/v). IR (ATR): 3273, 2950, 2808, 1711, 1547, 1309, 1222,

1053, 764, 690, 660, 505 cm^{-1}. ^{1}H-NMR ($CDCl_3$): δ 1.36–1.46 (m, 2H), 1.65–1.74 (m, 1H), 1.76–1.80 (m, 2H), 2.19–2.25 (m, 3H), 2.90–2.94 (m, 2H), 3.31 (d, *J* = 2.5 Hz, 2H), 4.04 (d, *J* = 6.4 Hz, 2H), 6.62 (bd, 1H), 7.04–7.08 (m, 1H), 7.28–7.38 (m, 4H). ^{13}C-NMR ($CDCl_3$): δ 28.56, 34.85, 46.97, 51.72, 69.18, 72.98, 78.81, 118.53, 123.19, 128.83, 137.79, 153.56. HRMS (ESI+): *m/z* calcd for $C_{16}H_{21}O_2N_2$ 273.1598; found 273.1591. UPLC purity, 98% at 254 nm (method A, t_R = 2.180 min).

Synthesis of (1-(prop-2-yn-1-yl)piperidin-3-yl)methyl phenylcarbamate (7)

Synthesized from (1-(prop-2-yn-1-yl)piperidin-3-yl)methanol (**47**) (0.238 g, 1.553 mmol, 1.0 equiv.), phenyl isocyanate (0.203 mL, 1.864 mmol, 1.2 equiv.) and 4-DMAP (0.019 g, 0.155 mmol, 0.1 equiv.) in CH_2Cl_2 (5 mL) via general procedure 1. The crude product was purified by flash column chromatography using EtOAc/*n*-hexane (3:2, v/v) as the eluent, to produce 0.383 g of **7** as a colourless oil which solidified into a white solid after cooling (89% yield). R_f = 0.30 (EtOAc/*n*-hexane, 2:1, v/v). IR (ATR): 3338, 3265, 2939, 1697, 1525, 1443, 1230, 1059, 741, 675, 620cm^{-1}. ^{1}H-NMR ($CDCl_3$): δ 0.98–1.10 (m, 1H), 1.57–1.67 (m, 1H), 1.72–1.78 (m, 2H), 1.98–2.09 (m, 2H), 2.17–2.23 (m, 1H), 2.25 (t, *J* = 2.4 Hz, 1H), 2.79–2.83 (m, 1H), 2.89–2.96 (m, 1H), 3.33 (d, *J* = 2.5 Hz, 2H), 3.98–4.02 (m, 1H), 4.09–4.13 (m, 1H), 6.66 (bs, 1H), 7.04–7.08 (m, 1H), 7.28–7.33 (m, 2H), 7.38 (bd, J = 7.8 Hz, 2H). ^{13}C-NMR ($CDCl_3$): δ 24.43, 26.46, 35.80, 47.18, 52.45, 55.51, 67.68, 73.19, 78.68, 118.73, 123.20, 128.81, 137.82, 153.57. HRMS (ESI+): *m/z* calcd for $C_{16}H_{21}O_2N_2$ 273.1598; found 273.1591. UPLC purity, 97% at 254 nm (method A, t_R = 2.233 min).

Synthesis of 1-benzylpiperidin-4-yl phenylcarbamate (8)

Synthesized from 1-benzylpiperidin-4-ol (**48**) (0.209 g, 1.093 mmol, 1.0 equiv.), phenyl isocyanate (0.143 mL, 1.312 mmol, 1.2 equiv.) and 4-DMAP (0.013 g, 0.109 mmol, 0.1

equiv.) in CH_2Cl_2 (5 mL) via general procedure 1. The crude product was purified by flash column chromatography using EtOAc/*n*-hexane (1:1, v/v) as the eluent, to produce 0.254 g of **8** as a colourless oil which solidified into a white solid after cooling (75% yield). R_f = 0.38 (EtOAc/*n*-hexane, 2:1, v/v). IR (ATR): 2944, 2799, 1720, 1555, 1446, 1314, 1216, 1062, 743, 695, 514 cm^{-1}. ^{1}H-NMR ($CDCl_3$): δ 1.70–1.79 (m, 2H), 1.95 (bs, 2H), 2.27 (bt, *J* = 9.3 Hz, 2H), 2.72 (bs, 2H), 3.51 (s, 2H), 4.76–4.83 (m, 1H), 6.62 (bs, 1H), 7.05 (t, *J* = 7.3 Hz, 1H), 7.23–7.38 (m, 9H). ^{13}C-NMR ($CDCl_3$): δ 31.02, 50.71, 62.86, 71.19, 118.52, 123.15, 126.96, 128.12, 128.88, 129.03, 137.93, 138.18, 153.02. HRMS (ESI+): *m/z* calcd for $C_{19}H_{23}O_2N_2$ 311.1754; found 311.1748. UPLC purity, 96% at 254 nm (method A, t_R = 2.650 min).

Synthesis of 1-benzylpiperidin-3-yl phenylcarbamate (9)

Synthesized from 1-benzylpiperidin-3-ol (**49**) (0.248 g, 1.297 mmol, 1.0 equiv.), phenyl isocyanate (0.169 mL, 1.556 mmol, 1.2 equiv.) and 4-DMAP (0.016 g, 0.130 mmol, 0.1 equiv.) in CH_2Cl_2 (5 mL) via general procedure 1. The crude product was purified by flash column chromatography using THF/*n*-hexane (1:4, v/v) as the eluent, to produce 0.328 g of **9** as a colourless oil which solidified into a white solid after cooling (81% yield). R_f = 0.57 (EtOAc/*n*-hexane, 2:1, v/v). IR (ATR): 3283, 2950, 1687, 1544, 1446, 1239, 1053, 1030, 740, 692, 505 cm^{-1}. ^{1}H-NMR ($CDCl_3$): δ 1.49–1.66 (m, 2H), 1.75–1.82 (m, 1H), 1.86–1.91 (m, 1H), 2.27–2.39 (m, 2H), 2.48–2.52 (m, 1H), 2.77 (bd, *J* = 11.3 Hz, 1H), 3.56 (d, *J* = 2.6 Hz, 2H), 4.90 (septet, *J* = 3.7 Hz, 1H), 6.69 (bs, 1H), 7.03–7.07 (m, 1H), 7.22–7.33 (m, 7H), 7.37 (bd, *J* = 7.7 Hz, 2H). ^{13}C-NMR ($CDCl_3$): δ 22.45, 29.44, 52.80, 57.11, 62.88, 70.26, 118.48, 123.10, 126.98, 128.09, 128.86, 129.04, 137.51, 137.94, 152.91. HRMS (ESI+): *m/z* calcd for $C_{19}H_{23}O_2N_2$ 311.1754; found 311.1747. UPLC purity, 98% at 254 nm (method A, t_R = 2.713 min).

Synthesis of (1-benzylpiperidin-4-yl)methyl phenylcarbamate (10)

Synthesized from (1-benzylpiperidin-4-yl)methanol (**50**) (0.244 g, 1.189 mmol, 1.0 equiv.), phenyl isocyanate (0.155 mL, 1.427 mmol, 1.2 equiv.) and 4-DMAP (0.015 g, 0.119 mmol, 0.1 equiv.) in CH_2Cl_2 (5 mL) via general procedure 1. The crude product was purified by flash column chromatography using THF/*n*-hexane (1:3, v/v) as the eluent, to produce 0.290 g of **10** as a colourless oil which solidified into a white solid after cooling (71% yield). R_f = 0.28 (EtOAc/*n*-hexane, 2:1, v/v). IR (ATR): 3359, 2933, 1701, 1539, 1443, 1224, 1062, 741, 695, 654, 505 cm^{-1}. ^{1}H-NMR ($CDCl_3$): δ 1.32–1.42 (m, 2H), 1.64–1.73 (m, 3H), 1.97 (td, J_1 = 11.8 Hz, J_2 = 2.1 Hz, 2H), 2.91 (bd, J = 11.5 Hz, 2H), 3.50 (s, 2H), 4.03 (d, J = 6.0 Hz, 2H), 6.63 (bs, 1H), 7.03–7.07 (m, 1H), 7.22–7.32 (m, 7H), 7.37 (bs, J = 7.8 Hz, 2H). ^{13}C-NMR ($CDCl_3$): δ 28.66, 30.19, 35.37, 53.07, 63.27, 69.38, 118.54, 123.17, 126.84, 128.04, 128.85, 129.07, 137.86, 138.20, 153.65. HRMS (ESI+): *m/z* calcd for $C_{20}H_{25}O_2N_2$ 325.1911; found 325.1904. UPLC purity, 96% at 254 nm (method A, t_R = 2.750 min).

Synthesis of (1-benzylpiperidin-3-yl)methyl phenylcarbamate (11)

Synthesized from (1-benzylpiperidin-3-yl)methanol (**51**) (0.255 g, 1.218 mmol, 1.0 equiv.), phenyl isocyanate (0.162 mL, 1.462 mmol, 1.2 equiv.) and 4-DMAP (0.015 g, 0.122 mmol, 0.1 equiv.) in CH_2Cl_2 (5 mL) via general procedure 1. The crude product was purified by flash column chromatography using THF/*n*-hexane (4:13, v/v) as the eluent, to produce 0.348 g of **11** as a colourless oil which solidified into a white solid after cooling (82% yield). R_f = 0.32 (EtOAc/*n*-hexane, 2:1, v/v). IR (ATR): 3315, 2935, 1704, 1528, 1442, 1312, 1216, 1059, 748, 696, 505 cm^{-1}. ^{1}H-NMR ($CDCl_3$): δ 1.03–1.13 (m, 1H), 1.52–1.64 (m, 1H), 1.65–1.69 (m, 1H), 1.73–1.76 (m, 1H), 1.89 (bd, J = 11.8 Hz, 1H), 1.96–2.06 (m, 2H), 2.74 (bd, J = 11.2 Hz, 1H), 2.85 (bd, J = 11.9 Hz, 1H), 3.50 (q, J = 13.5 Hz, 2H), 4.01 (dd, J_1 = 10.7 Hz, J_2 = 7.4 Hz, 1H), 4.08 (dd, J_1 = 10.8 Hz, J_2 = 5.8 Hz, 1H), 6.60 (bs, 1H), 7.03–7.07 (m, 1H), 7.22–7.36 (m,

9H). ^{13}C-NMR ($CDCl_3$): δ 24.40, 25.48, 26.96, 30.20, 35.72, 53.87, 56.79, 63.41, 67.80, 118.60, 123.17, 126.84, 128.06, 128.85, 129.02, 137.90, 138.20, 153.63. HRMS (ESI+): *m/z* calcd for $C_{20}H_{25}O_2N_2$ 325.1911; found 325.1908. UPLC purity, 96 % at 254 nm (method A, t_R = 2.787 min).

Synthesis of 1-(2,3-dihydro-1H-inden-2-yl)piperidin-4-yl phenylcarbamate (12)

Synthesized from 1-(2,3-dihydro-1*H*-inden-2-yl)piperidin-4-ol (**52**) (0.201 g, 0.925 mmol, 1.0 equiv.), phenyl isocyanate (0.121 mL, 1.110 mmol, 1.2 equiv.) and 4-DMAP (0.012 g, 0.093 mmol, 0.1 equiv.) in CH_2Cl_2 (5 mL) via general procedure 1. The crude product was purified by flash column chromatography using EtOAc/*n*-hexane (14:8, v/v) as the eluent, to produce 0.215 g of **12** as a white solid (81% yield). R_f = 0.52 (EtOAc/*n*-hexane, 3:1, v/v). IR (ATR): 3332, 2935, 1724, 1531, 1216, 1056, 740, 693, 622, 509cm^{-1}. ^{1}H-NMR ($CDCl_3$): δ 1.76–1.85 (m, 2H), 2.02–2.06 (m, 2H), 2.37 (bt, *J* = 9.2 Hz, 2H), 2.84–2.93 (m, 4H), 3.09 (q, *J* = 7.5 Hz, 2H), 3.21 (p, *J* = 8.1 Hz, 1H), 4.82 (sept. *J* = 4.0 Hz, 1H), 6.62 (s, 1H), 7.06 (t, *J* = 7.3 Hz, 1H), 7.13–7.21 (m, 4H), 7.31 (t, *J* = 7.9 Hz, 2H), 7.38 (bd, *J* = 7.9 Hz, 2H). ^{13}C-NMR ($CDCl_3$): δ 31.06, 37.25, 49.03, 66.76, 71.09, 118.55, 123.32, 124.33, 126.38, 129.01, 137.88, 141.51, 152.95. HRMS (ESI+): *m/z* calcd for $C_{21}H_{25}O_2N_2$ 337.1911; found 337.1902. UPLC purity, 97% at 254 nm (method A, t_R = 2.870 min).

Synthesis of 1-(2,3-dihydro-1H-inden-2-yl)piperidin-3-yl phenylcarbamate (13)

Synthesized from 1-(2,3-dihydro-1*H*-inden-2-yl)piperidin-3-ol (**53**) (0.204 g, 0.939 mmol, 1.0 equiv.), phenyl isocyanate (0.123 mL, 1.127 mmol, 1.2 equiv.) and 4-DMAP (0.012 g, 0.094 mmol, 0.1 equiv.) in CH_2Cl_2 (5 mL) via general procedure 1. The crude product was purified by flash column chromatography using THF/*n*-hexane (2:5, v/v) as the eluent, to produce 0.251 g of **13** as a colourless oil which solidified into a white solid after cooling (79% yield).

R_f = 0.45 (THF/*n*-hexane, 1:2, v/v). IR (ATR): 3294, 2959, 1697, 1542, 1443, 1317, 1232, 1057, 734, 696, 505 cm^{-1}. ^{1}H-NMR ($CDCl_3$): δ 1.65 (bs, 2H), 1.86 (d, *J* = 9.0 Hz, 2H), 2.52 (bs, 3H), 2.76 (bd, *J* = 9.4 Hz, 1H), 2.92 (sext., *J* = 8.2 Hz, 2H), 3.03–3.11 (m, 2H), 3.24 (p, *J* = 8.0 Hz, 1H), 4.96 (bs, 1H), 6.82 (s, 1H), 7.05 (t, *J* = 7.3 Hz, 1H), 7.12–7.18 (m, 4H), 7.30 (t, *J* = 8.0 Hz, 2H), 7.38 (bd, *J* = 7.9 Hz, 2H). ^{13}C-NMR ($CDCl_3$): δ 22.23, 29.36, 36.59, 36.76, 51.37, 55.32, 66.70, 70.02, 118.39, 123.14, 124.23, 126.27, 128.89, 137.88, 141.33, 141.34, 152.86. HRMS (ESI+): *m/z* calcd for $C_{21}H_{25}O_2N_2$ 337.1911; found 337.1903. UPLC purity, 98% at 254 nm (method A, t_R = 2.907 min).

Synthesis of (1-(2,3-dihydro-1H-inden-2-yl)piperidin-4-yl)methyl phenylcarbamate (14)

Synthesized from (1-(2,3-dihydro-1*H*-inden-2-yl)piperidin-4-yl)methanol (**54**) (0.202 g, 0.873 mmol, 1.0 equiv.), phenyl isocyanate (0.114 mL, 1.048 mmol, 1.2 equiv.) and 4-DMAP (0.011 g, 0.087 mmol, 0.1 equiv.) in CH_2Cl_2 (5 mL) via general procedure 1. The crude product was purified by flash column chromatography using EtOAc/*n*-hexane (5:2, v/v) as the eluent, to produce 0.227 g of **14** as a white solid (74% yield). R_f = 0.34 (EtOAc/*n*-hexane, 3:1, v/v). IR (ATR): 3455, 2943, 2807, 1714, 1445, 1315, 1237, 1057, 735, 692, 505 cm^{-1}. ^{1}H-NMR ($CDCl_3$): δ 1.39–1.49 (m, 2H), 1.70–1.81 (m, 3H), 2.05 (t, *J* = 11.0 Hz, 2H), 2.90 (dd, J_1 = 14.9 Hz, J_2 = 8.6 Hz, 2H), 3.06–3.21 (m, 5H), 4.06 (d, *J* = 5.8 Hz, 2H), 6.61 (s, 1H), 7.06 (t, *J* = 7.3 Hz, 1H), 7.12–7.19 (m, 4H), 7.31 (t, *J* = 7.8 Hz, 2H), 7.38 (bd, *J* = 7.6 Hz, 2H). ^{13}C-NMR ($CDCl_3$): δ 28.46, 35.28, 36.98, 51.26, 66.92, 69.18, 118.49, 123.15, 124.19, 126.22, 128.82, 137.84, 141.36, 153.63. HRMS (ESI+): *m/z* calcd for $C_{22}H_{27}O_2N_2$ 351.2067; found 351.2061. UPLC purity, 97% at 254 nm (method A, t_R = 2.923 min).

Synthesis of (1-(2,3-dihydro-1H-inden-2-yl)piperidin-3-yl)methyl phenylcarbamate (15)

Synthesized from (1-(2,3-dihydro-1*H*-inden-2-yl)piperidin-3-yl)methanol (**55**) (0.201 g, 0.869 mmol, 1.0 equiv.), phenyl isocyanate (0.114 mL, 1.043 mmol, 1.2 equiv.) and 4-DMAP (0.011 g, 0.087 mmol, 0.1 equiv.) in CH_2Cl_2 (5 mL) via general procedure 1. The crude product was purified by flash column chromatography using EtOAc/*n*-hexane (1:1, v/v) as the eluent, to produce 0.269 g of **15** as a colourless oil which solidified into a white solid after cooling (88% yield). R_f = 0.39 (EtOAc/*n*-hexane, 2:1, v/v). IR (ATR): 3506, 3342, 2923, 1698, 1526, 1444, 1226, 1065, 738, 691, 505 cm^{-1}. ^{1}H-NMR ($CDCl_3$): δ 1.07 (qd, J_1 = 12.0 Hz, J_2 = 4.0 Hz, 1H), 1.58–1.70 (m, 1H), 1.73–1.80 (m, 1H), 1.86 (t, J = 10.7 Hz, 2H), 1.96–2.10 (m, 2H), 2.88–2.97 (m, 3H), 3.04–3.22 (m, 4H), 4.01 (dd, J_1 = 10.5 Hz, J_2 = 7.4 Hz, 1H), 4.11 (dd, J_1 = 10.5 Hz, J_2 = 5.6 Hz, 1H), 6.65 (s, 1H), 7.07 (t, J = 7.3 Hz, 1H), 7.12–7.19 (m, 4H), 7.31 (t, J = 7.8 Hz, 2H), 7.39 (bd, J = 7.4 Hz, 2H). ^{13}C-NMR ($CDCl_3$): δ 24.61, 27.12, 35.87, 36.75, 37.01, 51.98, 55.18, 67.11, 67.98, 118.65, 123.25, 124.21, 126.21, 128.86, 137.79, 141.43, 141.44, 153.57. HRMS (ESI+): *m/z* calcd for $C_{22}H_{27}O_2N_2$ 351.2067; found 351.2060. UPLC purity, 96% at 254 nm (method A, t_R = 3.003 min).

Synthesis of 1-(prop-2-yn-1-yl)piperidin-4-yl (4-isopropylphenyl)carbamate (16)

Synthesized from 1-(prop-2-yn-1-yl)piperidin-4-ol (**44**) (0.215 g, 1.545 mmol, 1.0 equiv.), 4-isopropylphenyl isocyanate (0.296 mL, 1.853 mmol, 1.2 equiv.) and 4-DMAP (0.019 g, 0.155 mmol, 0.1 equiv.) in CH_2Cl_2 (5 mL) via general procedure 1. The crude product was purified by flash column chromatography using EtOAc/*n*-hexane (2:1, v/v) as the eluent, to produce 0.443 g of **16** as a colourless oil which solidified into a white solid after cooling (95% yield). R_f = 0.29 (EtOAc/*n*-hexane, 2:1, v/v). IR (ATR): 3287, 2961, 2817, 1717, 1539, 1224, 1059, 847, 680, 648, 551 cm^{-1}. ^{1}H-NMR ($CDCl_3$): δ 1.23 (d, J = 6.9 Hz, 6H), 1.74–1.83 (m, 2H), 1.98–2.05 (m, 2H), 2.26 (t, J = 2.4 Hz, 1H), 2.44–2.49 (m, 2H), 2.77–2.92 (m, 3H), 3.32 (d, J = 2.4 Hz, 2H), 4.77–4.81 (m, 1H), 6.58 (bs, 1H), 7.16 (d, J = 8.5 Hz, 2H), 7.29 (bd, J = 8.0

Hz, 2H). ^{13}C-NMR ($CDCl_3$): δ 23.91, 30.88, 33.31, 46.73, 49.52, 70.31, 73.16, 78.65, 118.76, 126.73, 135.52, 143.82, 153.07. HRMS (ESI+): *m/z* calcd for $C_{18}H_{25}O_2N_2$ 301.1911; found 301.1906. UPLC purity, 98% at 254 nm (method A, t_R = 3.007 min).

Synthesis of 1-(prop-2-yn-1-yl)piperidin-3-yl (4-isopropylphenyl)carbamate (17)

Synthesized from 1-(prop-2-yn-1-yl)piperidin-3-ol (**45**) (0.203 g, 1.480 mmol, 1.0 equiv.), 4-isopropylphenyl isocyanate (0.279 mL, 1.776 mmol, 1.2 equiv.) and 4-DMAP (0.018 g, 0.148 mmol, 0.1 equiv.) in CH_2Cl_2 (5 mL) via general procedure 1. The crude product was purified by flash column chromatography using EtOAc/*n*-hexane (1:2, v/v) as the eluent, to produce 0.401 g of **17** as a colourless oil which solidified into a white solid after cooling (92% yield). R_f = 0.64 (EtOAc/*n*-hexane, 2:1, v/v). IR (ATR): 3342, 3277, 2951, 2803, 1686, 1526, 1234, 1069, 828, 640, 544 cm^{-1}. ^{1}H-NMR ($CDCl_3$): δ 1.22 (d, *J* = 6.9 Hz, 6H), 1.60–1.70 (m, 2H), 1.79–1.92 (m, 2H), 2.26 (t, *J* = 2.4 Hz, 1H), 2.50–2.60 (m, 2H), 2.63–2.67 (m, 1H), 2.78 (bd, *J* = 10.2 Hz, 1H), 2.86 (sept., *J* = 6.9 Hz, 1H), 3.38 (d, *J* = 2.5 Hz, 2H), 4.95–5.00 (m, 1H), 6.72 (bs, 1H), 7.14–7.17 (m, 2H), 7.29 (bd, *J* = 8.4 Hz, 2H). ^{13}C-NMR ($CDCl_3$): δ 21.84, 23.90, 28.50, 33.31, 46.89, 51.60, 55.58, 69.64, 73.53, 78.05, 118.62, 126.73, 135.52, 143.77, 152.95. HRMS (ESI+): *m/z* calcd for $C_{18}H_{25}O_2N_2$ 301.1911; found 301.1905. UPLC purity, 98% at 254 nm (method A, t_R = 3.010 min).

Synthesis of (1-(prop-2-yn-1-yl)piperidin-4-yl)methyl (4-isopropylphenyl)carbamate (18)

Synthesized from (1-(prop-2-yn-1-yl)piperidin-4-yl)methanol (**46**) (0.216, 1.410 mmol, 1.0 equiv.), 4-isopropylphenyl isocyanate (0.270 mL, 1.692 mmol, 1.2 equiv.) and 4-DMAP (0.017 g, 0.141 mmol, 0.1 equiv.) in CH_2Cl_2 (5 mL) via general procedure 1. The crude product was purified by flash column chromatography using EtOAc/*n*-hexane (2:1, v/v) as the eluent, to produce 0.425 g of **18** as a colourless oil which solidified into a white solid after

cooling (96% yield). R_f = 0.28 (EtOAc/*n*-hexane, 2:1, v/v). IR (ATR): 3255, 2960, 2903, 1713, 1543, 1307, 1220, 1043, 829, 768, 545 cm^{-1}. ^{1}H-NMR ($CDCl_3$): δ 1.23 (d, *J* = 6.9 Hz, 6H), 1.35–1.45 (m, 2H), 1.64–1.73 (m, 1H), 1.78 (bd, *J* = 13.6 Hz, 2H), 2.18–2.25 (m, 3H), 2.81–2.93 (m, 3H), 3.31 (d, *J* = 2.4 Hz, 2H), 4.03 (d, *J* = 6.3 Hz, 2H), 6.60 (bs, 1H), 7.16 (d, *J* = 8.4 Hz, 2H), 7.28 (bd, *J* = 7.5 Hz, 2H). ^{13}C-NMR ($CDCl_3$): δ 23.90, 28.60, 33.30, 34.89, 46.99, 51.74, 69.10, 72.96, 78.82, 118.74, 126.72, 135.45, 143.86, 153.71. HRMS (ESI+): *m/z* calcd for $C_{19}H_{27}O_2N_2$ 315.2067; found 315.2062. UPLC purity, 97% at 254 nm (method A, t_R = 3.080 min).

Synthesis of (1-(prop-2-yn-1-yl)piperidin-3-yl)methyl (4-isopropylphenyl)carbamate (19)

Synthesized from (1-(prop-2-yn-1-yl)piperidin-3-yl)methanol (**47**) (0.218 g, 1.423 mmol, 1.0 equiv.), 4-isopropylphenyl isocyanate (0.273 mL, 1.707 mmol, 1.2 equiv.) and 4-DMAP (0.017 g, 0.142 mmol, 0.1 equiv.) in CH_2Cl_2 (5 mL) via general procedure 1. The crude product was purified by flash column chromatography using EtOAc/*n*-hexane (1:1, v/v) as the eluent, to produce 0.425 g of **19** as a colourless oil which solidified into a white solid after cooling (95% yield). R_f = 0.36 (EtOAc/*n*-hexane, 2:1, v/v). IR (ATR): 3348, 3274, 2936, 1698, 1524, 1309, 1232, 1065, 831, 650, 541 cm^{-1}. ^{1}H-NMR ($CDCl_3$): δ 0.98–1.09 (m, 1H), 1.23 (d, *J* = 7.0 Hz, 6H), 1.57–1.66 (m, 1H), 1.72–1.77 (m, 2H), 1.99–2.05 (m, 2H), 2.18 (qd, J_1 = 11.3 Hz, J_2 = 2.3 Hz, 1H), 2.25 (t, *J* = 2.4 Hz, 1H), 2.80–2.96 (m, 3H), 3.33 (d, *J* = 2.4 Hz, 2H), 4.0 (dd, J_1 = 10.8 Hz, J_2 = 6.8 Hz, 1H), 4.10 (dd, J_1 = 10.9 Hz, J_2 = 5.0 Hz, 1H), 6.58 (bs, 1H), 7.16 (d, *J* = 8.5 Hz, 2H), 7.29 (db, *J* = 7.2 Hz, 2H). ^{13}C-NMR ($CDCl_3$): δ 23.91, 24.49, 26.51, 33.32, 35.88, 47.22, 52.49, 55.56, 67.63, 73.15, 78.72, 118.88, 126.72, 135.48, 143.87, 153.70. HRMS (ESI+): *m/z* calcd $C_{19}H_{27}O_2N_2$ 315.2067; found 315.2063. UPLC purity, 98% at 254 nm (method A, t_R = 3.100 min).

Synthesis of 1-benzylpiperidin-4-yl (4-isopropylphenyl)carbamate (20)

Synthesized from 1-benzylpiperidin-4-ol (**48**) (0.251 g, 1.312 mmol, 1.0 equiv.), 4-isopropylphenyl isocyanate (0.251 mL, 1.575 mmol, 1.2 equiv.) and 4-DMAP (0.016 g, 0.131 mmol, 0.1 equiv.) in CH_2Cl_2 (5 mL) via general procedure 1. The crude product was purified by flash column chromatography using EtOAc/*n*-hexane (4:7, v/v) as the eluent, to produce 0.420 g of **20** as a white solid (91% yield). R_f = 0.38 (EtOAc/*n*-hexane, 1:1, v/v). IR (ATR): 3357, 2957, 1693, 1524, 1310, 1231, 1062, 825, 742, 664, 541 cm^{-1}. ^{1}H-NMR ($CDCl_3$): δ 1.22 (d, *J* = 6.9 Hz, 6H), 1.70–1.78 (m, 2H), 1.94–1.99 (m, 2H), 2.27 (bt, *J* = 9.3 Hz, 2H), 2.70–2.73 (m, 2H), 2.86 (sept., *J* = 6.9 Hz, 1H), 3.51 (s, 2H), 4.75–4.83 (m, 1H), 6.55 (bs, 1H), 7.16 (d, *J* = 8.4 Hz, 2H), 7.23–7.32 (m, 7H). ^{13}C-NMR ($CDCl_3$): δ 23.96, 31.05, 33.36, 50.75, 62.89, 71.12, 118.74, 126.77, 126.95, 128.13, 129.02, 135.59, 138.21, 143.80, 153.17. HRMS (ESI+): *m/z* calcd for $C_{22}H_{29}O_2N_2$ 353.2224; found 353.2217. UPLC purity, 98% at 254 nm (method A, t_R = 3.373 min).

Synthesis of 1-benzylpiperidin-3-yl (4-isopropylphenyl)carbamate (21)

Synthesized from 1-benzylpiperidin-3-ol (**49**) (0.236 g, 1.234 mmol, 1.0 equiv.), 4-isopropylphenyl isocyanate (0.236 mL, 1.481 mmol, 1.2 equiv.) and 4-DMAP (0.015 g, 0.123 mmol, 0.1 equiv.) in CH_2Cl_2 (5 mL) via general procedure 1. The crude product was purified by flash column chromatography using THF/*n*-hexane (1:5, v/v) as the eluent, to produce 0.381 g of **21** as a colourless oil which solidified into a white solid after cooling (88% yield). R_f = 0.47 (THF/*n*-hexane, 1:2, v/v). IR (ATR): 3364, 2950, 1698, 1523, 1220, 1054, 826, 735, 678, 641, 543 cm^{-1}. ^{1}H-NMR ($CDCl_3$): δ 1.22 (d, *J* = 6.9 Hz, 6H), 1.48–1.65 (m, 2H), 1.74–1.82 (m, 1H), 1.84–1.91 (m, 1H), 2.26–2.39 (m, 2H), 2.48–2.52 (m, 1H), 2.77 (db, *J* = 11.2 Hz, 1H), 2.86 (sept., *J* = 6.9 Hz, 1H), 3.56 (d, *J* = 3.0 Hz, 2H), 4.89 (sept. *J* = 3.6 Hz, 1H), 6.60 (bs, 1H), 7.14–7.17 (m, 2H), 7.22–7.33 (m, 7H). ^{13}C-NMR ($CDCl_3$): δ 22.47, 23.95,

29.47, 33.36, 52.82, 57.17, 62.91, 70.17, 118.70, 126.76, 126.97, 128.09, 129.05, 135.59, 137.55, 143.76, 153.05. HRMS (ESI+): *m/z* calcd for $C_{22}H_{29}O_2N_2$ 353.2224; found 353.2218. UPLC purity, 98% at 254 nm (method A, t_R = 3.433 min).

Synthesis of (1-benzylpiperidin-4-yl)methyl (4-isopropylphenyl)carbamate (22)

Synthesized from (1-benzylpiperidin-4-yl)methanol (**50**) (0.266 g, 1.296 mmol, 1.0 equiv.), 4-isopropylphenyl isocyanate (0.248 mL, 1.555 mmol, 1.2 equiv.) and 4-DMAP (0.016 g, 0.130 mmol, 0.1 equiv.) in CH_2Cl_2 (5 mL) via general procedure 1. The crude product was purified by flash column chromatography using EtOAc/*n*-hexane (4:7, v/v) as the eluent, to produce 0.423 g of **22** as a colourless oil which solidified into a white solid after cooling (89% yield). R_f = 0.26 (EtOAc/*n*-hexane, 2:1, v/v). IR (ATR): 3356, 2954, 1700, 1521, 1224, 1057, 825, 743, 698, 621, 543 cm^{-1}. ^{1}H-NMR ($CDCl_3$): δ 1.22 (d, J = 7.0 Hz, 6H), 1.31–1.41 (m, 2H), 1.71 (d, *J* = 11.3 Hz, 3H), 1.93–1.99 (m, 2H), 2.81–2.92 (m, 3H), 3.50 (s, 2H), 4.02 (d, *J* = 5.9 Hz, 2H), 6.56 (bs, 1H), 7.16 (d, *J* = 8.4 Hz, 2H), 7.22–7.32 (m, 7H). ^{13}C-NMR ($CDCl_3$): δ 23.95, 28.68, 33.34, 35.42, 53.10, 63.29, 69.32, 118.74, 126.76, 126.86, 128.05, 129.09, 135.52, 138.21, 143.85, 153.78. HRMS (ESI+): *m/z* calcd for $C_{23}H_{31}O_2N_2$ 367.2380; found 367.2376. UPLC purity, 98% at 254 nm (method A, t_R = 3.453 min).

Synthesis of (1-benzylpiperidin-3-yl)methyl (4-isopropylphenyl)carbamate (23)

Synthesized from (1-benzylpiperidin-4-yl)methanol (**51**) (0.237 g, 1.154 mmol, 1.0 equiv.), 4-isopropylphenyl isocyanate (0.221 mL, 1.385 mmol, 1.2 equiv.) and 4-DMAP (0.014 g, 0.115 mmol, 0.1 equiv.) in CH_2Cl_2 (5 mL) via general procedure 1. The crude product was purified by flash column chromatography using EtOAc/*n*-hexane (4:7, v/v) as the eluent, to produce 0.381 g of **23** as a colourless oil (90% yield). R_f = 0.41 (EtOAc/*n*-hexane, 2:1, v/v). IR (ATR): 3317, 2935, 1702, 1524, 1312, 1219, 1063, 832, 740, 699, 546 cm^{-1}. ^{1}H-NMR ($CDCl_3$): δ

1.02–1.12 (m, 1H), 1.22 (d, *J* = 6.9 Hz, 6H), 1.52–1.63 (m, 1H), 1.64–1.73 (m, 2H), 1.86 (bt, *J* = 10.2 Hz, 1H), 1.95–2.03 (m, 2H), 2.74 (bd, *J* = 11.2 Hz, 1H), 2.86 (sept., *J* = 6.9 Hz, 2H), 3.49 (q, *J* = 13.5 Hz, 2H), 3.99 (dd, J_1 = 10.8, J_2 = 7.4 Hz, 1H), 4.07 (dd, J_1 = 10.8, J_2 = 5.8 Hz, 1H), 6.55 (bd, 1H), 7.15 (d, *J* = 8.4 Hz, 2H), 7.21–7.32 (m, 7H). ^{13}C-NMR ($CDCl_3$): δ 23.95, 24.43, 26.98, 33.36, 35.76, 53.88, 56.83, 63.42, 67.72, 118.79, 126.74, 126.83, 128.06, 129.02, 135.53, 138.24, 143.84, 153.75. HRMS (ESI+): *m/z* calcd for $C_{23}H_{31}O_2N_2$ 367.2380; found 367.2374. UPLC purity, 98% at 254 nm (method A, t_R = 3.480 min).

Synthesis of 1-(2,3-dihydro-1H-inden-2-yl)piperidin-4-yl (4-isopropylphenyl)carbamate (24)

Synthesized from 1-(2,3-dihydro-1*H*-inden-2-yl)piperidin-4-ol (**52**) (0.202 g, 0.930 mmol, 1.0 equiv.), 4-isopropylphenyl isocyanate (0.178 mL, 1.115 mmol, 1.2 equiv.) and 4-DMAP (0.012 g, 0.093 mmol, 0.1 equiv.) in CH_2Cl_2 (5 mL) via general procedure 1. The crude product was purified by flash column chromatography using EtOAc/*n*-hexane (1:1, v/v) as the eluent, to produce 0.213 g of **24** as a white solid (61% yield). R_f = 0.30 (EtOAc/*n*-hexane, 1:1, v/v). IR (ATR): 3234, 2955, 1720, 1603, 1542, 1312, 1219, 1052, 817, 745, 540 cm^{-1}. ^{1}H-NMR ($CDCl_3$): δ 1.23 (d, *J* = 6.9 Hz, 6H), 1.76–1.84 (m, 2H), 2.01–2.05 (m, 2H), 2.37 (bt, J = 8.2 Hz, 2H), 2.83–2.93 (m, 5H), 3.09 (q, *J* = 7.5 Hz, 2H), 3.20 (p, *J* = 8.0 Hz, 1H), 4.81 (bs, 1H), 6.59 (s, 1H), 7.13–7.20 (m, 6H), 7.29 (bs, *J* = 7.7 Hz, 2H). ^{13}C-NMR ($CDCl_3$): δ 24.01, 31.05, 33.43, 37.25, 49.07, 66.77, 70.96, 118.74, 124.33, 126.36, 126.87, 135.54, 141.51, 143.98, 153.10. HRMS (ESI+): *m/z* calcd for $C_{24}H_{31}O_2N_2$ 379.2380; found 379.2374. UPLC purity, 98% at 254 nm (method, t_R = 3.523 min).

Synthesis of 1-(2,3-dihydro-1H-inden-2-yl)piperidin-3-yl (4-isopropylphenyl)carbamate (25)

Synthesized from 1-(2,3-dihydro-1*H*-inden-2-yl)piperidin-3-ol (**53**) (0.201 g, 0.925 mmol, 1.0 equiv.), 4-isopropylphenyl isocyanate (0.177 mL, 1.111 mmol, 1.2 equiv.) and 4-DMAP (0.012 g, 0.093 mmol, 0.1 equiv.) in CH_2Cl_2 (5 mL) via general procedure 1. The crude product was purified by flash column chromatography using EtOAc/*n*-hexane (1:2, v/v) as the eluent, to produce 0.301 g of **25** as a colourless oil which solidified into a white solid after cooling (85% yield). R_f = 0.36 (THF/*n*-hexane, 1:1, v/v). IR (ATR): 3310, 2958, 1696, 1535, 1318, 1239, 1064, 829, 743, 689, 543 cm^{-1}. ^{1}H-NMR ($CDCl_3$): δ 1.22 (d, *J* = 6.9 Hz, 6H), 1.65 (bs, 2H), 1.86 (bd, *J* = 8.9 Hz, 2H), 2.53 (bs, 3H), 2.76 (bd, *J* = 9.2 Hz, 1H), 2.83–2.98 (m, 3H), 3.03–3.11 (m, 2H), 3.24 (p, *J* = 8.0 Hz, 1H), 4.95 (bs, 1H), 6.69 (s, 1H), 7.12–7.18 (m, 6H), 7.29 (bs, *J* = 8.0 Hz, 2H). ^{13}C-NMR ($CDCl_3$): δ 22.24, 23.94, 29.37, 33.34, 36.60, 36.77, 51.39, 55.36, 66.72, 69.88, 118.64, 124.23, 126.27, 126.76, 135.54, 141.34, 141.36, 143.79, 153.01. HRMS (ESI+): *m/z* calcd for $C_{24}H_{31}O_2N_2$ 379.2380; found 379.2373. UPLC purity, 96% at 254 nm (method A, t_R = 3.570 min).

Synthesis of (1-(2,3-dihydro-1H-inden-2-yl)piperidin-4-yl)methyl (4-isopropylphenyl)carbamate (26)

Synthesized from (1-(2,3-dihydro-1*H*-inden-2-yl)piperidin-4-yl)methanol (**54**) (0.201 g, 0.869 mmol, 1.0 equiv.), 4-isopropylphenyl isocyanate (0.166 mL, 1.043 mmol, 1.2 equiv.) and 4-DMAP (0.011 g, 0.087 mmol, 0.1 equiv.) in CH_2Cl_2 (5 mL) via general procedure 1. The crude product was purified by flash column chromatography using EtOAc/*n*-hexane (14:8, v/v) as the eluent, to produce 0.283 g of **26** as a white solid (83% yield). R_f = 0.34 (EtOAc/*n*-hexane, 2:1, v/v). IR (ATR): 3278, 2952, 1691, 1536, 1309, 1245, 1059, 827, 747, 679, 542 cm^{-1}. ^{1}H-NMR ($CDCl_3$): δ 1.22 (d, *J* = 6.9 Hz, 6H), 1.38–1.47 (m, 2H), 1.67–1.79 (m, 3H), 2.04 (bt, *J* = 11.0 Hz, 2H), 2.81–2.93 (m, 3H), 3.05–3.21 (m, 5H), 4.04 (d, *J* = 5.9 Hz, 2H), 6.62 (s, 1H), 7.12–7.19 (m, 6H), 7.29 (bd, *J* = 7.0 Hz, 2H). ^{13}C-NMR ($CDCl_3$): δ 23.92, 28.62,

33.31, 35.35, 37.06, 51.29, 66.98, 69.22, 118.72, 124.21, 126.21, 126.74, 135.44, 141.44, 143.85, 153.69. HRMS (ESI+): *m/z* calcd for $C_{25}H_{33}O_2N_2$ 393.2537; found 393.2528. UPLC purity, 98% at 254 nm (method A, t_R = 3.570 min).

Synthesis of (1-(2,3-dihydro-1H-inden-2-yl)piperidin-3-yl)methyl (4-isopropylphenyl)carbamate (27)

Synthesized from (1-(2,3-dihydro-1*H*-inden-2-yl)piperidin-3-yl)methanol (**55**) (0.200 g, 0.865 mmol, 1.0 equiv.), 4-isopropylphenyl isocyanate (0.166 mL, 1.037 mmol, 1.2 equiv.) and 4-DMAP (0.011 g, 0.087 mmol, 0.1 equiv.) in CH_2Cl_2 (5 mL) via general procedure 1. The crude product was purified by flash column chromatography using EtOAc/*n*-hexane (3:2, v/v) as the eluent, to produce 0.325 g of **27** as a colourless oil which solidified into a white solid after cooling (96% yield). R_f = 0.41 (EtOAc/*n*-hexane, 2:1, v/v). IR (ATR): 3344, 2963, 2927, 1670, 1528, 1227, 1066, 828, 737, 632, 544 cm^{-1}. ^{1}H-NMR ($CDCl_3$): δ 1.01–1.11 (m, 1H), 1.23 (d, *J* = 6.9 Hz, 6H), 1.58–1.69 (m, 1H), 1.73–1.80 (m, 2H), 1.85 (t, *J* = 10.6 Hz, 1H), 1.97–2.04 (m, 2H), 2.82–2.96 (m, 4H), 3.03–3.22 (m, 4H), 4.00 (dd, J_1 = 10.2 Hz, J_2 = 7.6 Hz, 1H), 4.10 (dd, J_1 = 10.1 Hz, J_2 = 5.2 Hz, 1H), 6.60 (s, 1H), 7.12–7.18 (m, 6H), 7.30 (db, *J* = 5.8 Hz, 2H). ^{13}C-NMR ($CDCl_3$): δ 23.94, 24.65, 27.14, 33.34, 35.92, 36.80, 37.05, 52.03, 55.25, 67.14, 67.91, 118.78, 124.23, 126.22, 126.76, 135.45, 141.46, 141.47, 143.93, 153.66. HRMS (ESI+): *m/z* calcd for $C_{25}H_{33}O_2N_2$ 393.2537; found 393.2527. UPLC purity, 98% at 254 nm (method A, t_R = 3.633 min).

Synthesis of 1-(prop-2-yn-1-yl)piperidin-4-yl ethyl(methyl)carbamate (28)

Synthesized from 1-(prop-2-yn-1-yl)piperidin-4-ol (**44**) (0.201 g, 1.444 mmol, 1.0 equiv.) and *N*-ethyl-*N*-methylcarbamoyl chloride (0.191 mL, 1.733 mmol, 1.2 equiv.) in pyridine (5 mL). The crude product was purified by flash column chromatography using CH_2Cl_2/MeOH (30:1,

v/v) as the eluent, to produce 0.118 g of **28** as a slightly orange oil (36% yield). R_f = 0.43 (CH_2Cl_2/MeOH, 9:1, v/v). IR (ATR): 3239, 2937, 2808, 1687, 1400, 1285, 1177, 1089, 1053, 1034, 769, 622 cm^{-1}. ^{1}H-NMR ($CDCl_3$): δ 1.11 (t, *J* = 7.1 Hz, 3H), 1.72–1.80 (m, 2H), 1.91–1.98 (m, 2H), 2.25 (t, *J* = 2.5 Hz, 1H), 2.48 (bt, *J* = 8.1 Hz, 2H), 2.74 (bs, 2H), 2.89 (s, 3H), 3.31 (d, *J* = 2.4 Hz, 4H), 4.74 (bs, 1H). ^{13}C-NMR ($CDCl_3$): δ 12.33, 12.75, 30.79, 32.93, 33.61, 43.22, 46.74, 49.08, 69.40, 72.89, 78.59, 155.31. HRMS (ESI+): *m/z* calcd for $C_{12}H_{21}O_2N_2$ 225.1598; found 225.1596.

Synthesis of 1-(prop-2-yn-1-yl)piperidin-3-yl ethyl(methyl)carbamate (29)

Synthesized from 1-(prop-2-yn-1-yl)piperidin-3-ol (**45**) (0.213 g, 1.530 mmol, 1.0 equiv.) and *N*-ethyl-*N*-methylcarbamoyl chloride (0.203 mL, 1.836 mmol, 1.2 equiv.) in pyridine (5 mL). The crude product was purified by flash column chromatography using CH_2Cl_2/MeOH (50:1, v/v) as the eluent, to produce 0.132 g of **29** as a slightly orange oil (38% yield). R_f = 0.50 (CH_2Cl_2/MeOH, 30:1, v/v). IR (ATR): 3242, 2940, 2803, 1690, 1400, 1261, 1176, 1102, 1086, 769, 622 cm^{-1}. ^{1}H-NMR ($CDCl_3$): δ 1.10 (t, J = 7.1 Hz, 3H), 1.34–1.43 (m, 1H), 1.57–1.68 (m, 1H), 1.74–1.82 (m, 1H), 1.89–1.95 (m, 1H), 2.25 (t, *J* = 2.5 Hz, 1H), 2.30–2.35 (m, 2H), 2.62–2.66 (m, 1H), 2.88–2.93 (m, 4H), 3.31 (bs, 2H), 3.36 (d, *J* = 2.4 Hz, 2H), 4.78 (sept., *J* = 4.2 Hz, 1H). ^{13}C-NMR ($CDCl_3$): δ 12.70, 22.56, 29.30, 33.58, 43.20, 46.69, 51.40, 55.96, 69.88, 73.16, 78.24, 155.33. HRMS (ESI+): *m/z* calcd for $C_{12}H_{21}O_2N_2$ 225.1598; found 225.1597.

Synthesis of (1-(prop-2-yn-1-yl)piperidin-4-yl)methyl ethyl(methyl)carbamate (30)

Synthesized from (1-(prop-2-yn-1-yl)piperidin-4-yl)methanol (**46**) (0.200 g, 1.305 mmol, 1.0 equiv.) and *N*-ethyl-*N*-methylcarbamoyl chloride (0.173 mL, 1.566 mmol, 1.2 equiv.) in pyridine (5 mL) via general procedure 2. The crude product was purified by flash column

chromatography using CH_2Cl_2/MeOH (30:1, v/v) as the eluent, to produce 0.132 g of **30** as a slightly orange oil (40% yield). R_f = 0.41 (CH_2Cl_2/MeOH, 15:1, v/v). IR (ATR): 3235, 2935, 2803, 1693, 1403, 1283, 1177, 1087, 984, 770, 624 cm^{-1}. ^{1}H-NMR ($CDCl_3$): δ 1.11 (t, J = 7.1 Hz, 3H), 1.39 (qd, J_1 = 12.2 Hz, J_2 = 3.5 Hz, 2H), 1.61–1.69 (m, 1H), 1.76 (bd, J = 12.9 Hz, 2H), 2.18–2.25 (m, 3H), 2.89–2.92 (m, 5H), 3.31 (d, J = 2.5 Hz, 4H), 3.94 (d, J = 6.4 Hz, 2H). ^{13}C-NMR ($CDCl_3$): δ 12.81, 28.48, 28.59, 34.92, 43.12, 43.31, 46.54, 46.91, 51.72, 69.18, 72.83, 78.70, 155.97. HRMS (ESI+): *m/z* calcd for $C_{13}H_{23}O_2N_2$ 239.1754; found 239.1753.

Synthesis of (1-(prop-2-yn-1-yl)piperidin-3-yl)methyl ethyl(methyl)carbamate (31)

Synthesized from (1-(prop-2-yn-1-yl)piperidin-3-yl)methanol (**47**) (0.201 g, 1.312 mmol, 1.0 equiv.) and *N*-ethyl-*N*-methylcarbamoyl chloride (0.174 mL, 1.574 mmol, 1.2 equiv.) in pyridine (5 mL) via general procedure 2. The crude product was purified by flash column chromatography using CH_2Cl_2/MeOH (20:1, v/v) as the eluent, to produce 0.103 g of **31** as a slightly orange oil (33% yield). R_f = 0.55 (CH_2Cl_2/MeOH, 9:1, v/v). IR (ATR): 3240, 2934, 2800, 1693, 1403, 1285, 1176, 1083, 984, 769, 622 cm^{-1}. ^{1}H-NMR ($CDCl_3$): δ 0.95–1.06 (m, 1H), 1.11 (t, J = 7.2 Hz, 3H), 1.56–1.67 (m, 1H), 1.70–1.75 (m, 2H), 1.96–2.02 (m, 2H), 2.17 (td, J_1 = 11.3 Hz, J_2 = 2.7 Hz, 1H), 2.24 (t, J = 2.5 Hz, 1H), 2.80–2.96 (m, 5H), 3.25–3.32 (m, 4H), 3.89 (bs, 1H), 4.01 (dd, J_1 = 10.8 Hz, J_2 = 4.9 Hz, 1H). ^{13}C-NMR ($CDCl_3$): δ 12.83, 24.54, 26.50, 33.69, 43.19, 43.36, 47.17, 52.47, 55.62, 67.65, 72.89, 78.67, 155.90. HRMS (ESI+): *m/z* calcd for $C_{13}H_{23}O_2N_2$ 239.1754; found 239.1753.

Synthesis of 1-benzylpiperidin-4-yl ethyl(methyl)carbamate (32)

Synthesized from 1-benzylpiperidin-4-ol (**48**) (0.202 g, 1.056 mmol, 1.0 equiv.) and *N*-ethyl-*N*-methylcarbamoyl chloride (0.140 mL, 1.267 mmol, 1.2 equiv.) in pyridine (5 mL) via general procedure 2. The crude product was purified by flash column chromatography using

CH_2Cl_2/MeOH (30:1, v/v) as the eluent, to produce 0.098 g of **32** as a slightly orange oil (34% yield). R_f = 0.31 (CH_2Cl_2/MeOH, 20:1, v/v). IR (ATR): 2937, 2801, 1693, 1453, 1399, 1285, 1177, 1054, 1031, 739, 699 cm^{-1}. ^{1}H-NMR ($CDCl_3$): δ 1.10 (t, J = 7.1 Hz, 3H), 1.66–1.75 (m, 2H), 1.87–1.94 (m, 2H), 2.30 (bs, 2H), 2.64 (bs, 2H), 2.87 (s, 3H), 3.29 (bs, 2H), 3.50 (s, 2H), 4.69–4.74 (m, 1H), 7.21–7.33 (m, 5H). ^{13}C-NMR ($CDCl_3$): δ 12.47, 12.83, 31.09, 33.02, 33.69, 43.31, 50.62, 62.95, 70.36, 126.84, 128.05, 128.93, 138.36, 155.56. HRMS (ESI+): *m/z* calcd for $C_{19}H_{25}O_2N_2$ 277.1911; found 277.1912. UPLC purity, 98% at 210 nm (method A, t_R = 2.277 min).

Synthesis of 1-benzylpiperidin-3-yl ethyl(methyl)carbamate (33)

Synthesized from 1-benzylpiperidin-3-ol (**49**) (0.202 g, 1.056 mmol, 1.0 equiv.) and *N*-ethyl-*N*-methylcarbamoyl chloride (0.140 mL, 1.267 mmol, 1.2 equiv.) in pyridine (5 mL) via general procedure 2. The crude product was purified by flash column chromatography using CH_2Cl_2/MeOH (35:1, v/v) as the eluent, to produce 0.108 g of **33** slightly orange oil (37% yield). R_f = 0.40 (CH_2Cl_2/MeOH, 30:1, v/v). IR (ATR): 2940, 2796, 1693, 1453, 1399, 1261, 1178, 1086, 972, 769, 739, 699 cm^{-1}. ^{1}H-NMR ($CDCl_3$): δ 1.10 (t, J = 7.2 Hz, 3H), 1.42 (bs, 1H), 1.54–1.64 (m, 1H), 1.69–1.77 (m, 1H), 1.90 (bs, 1H), 2.13–2.18 (m, 2H), 2.56 (bs, 1H), 2.79–2.87 (m, 4H), 3.29 (bs, 2H), 3.52 (dd, J_1 = 20.3 Hz, J_2 = 13.4 Hz, 2H), 4.77 (bs, 1H), 7.20–7.31 (m, 5H). ^{13}C-NMR ($CDCl_3$): δ 12.84, 22.82, 29.91, 33.71, 43.31, 52.98, 57.51, 62.71, 70.06, 126.78, 128.02, 128.71, 138.26, 155.56. HRMS (ESI+): *m/z* calcd for $C_{16}H_{25}0_2N_2$ 277.1911; found 277.1912. UPLC purity, 95% at 210 nm (method A, t_R = 2.670 min).

Synthesis of (1-benzylpiperidin-4-yl)methyl ethyl(methyl)carbamate (34)

Synthesized from (1-benzylpiperidin-4-yl)methanol (**50**) (0.203 g, 0.989 mmol, 1.0 equiv.) and *N*-ethyl-*N*-methylcarbamoyl chloride (0.131 mL, 1.187 mmol, 1.2 equiv.) in pyridine (5 mL) via general procedure 2. The crude product was purified by flash column chromatography using CH_2Cl_2/MeOH (20:1, v/v) as the eluent, to produce 0.115 g of **34** as a slightly orange oil (40% yield). R_f = 0.27 (CH_2Cl_2/MeOH, 20:1, v/v). IR (ATR): 2935, 2799, 2757, 1697, 1402, 1283, 1176, 1086, 983, 739, 699 cm^{-1}. ^{1}H-NMR ($CDCl_3$): δ 1.10 (t, J = 7.1 Hz, 3H), 1.35 (qd, J_1 = 11.7 Hz, J_2 = 3.0 Hz, 2H), 1.60–1.70 (m, 3H), 1.97 (td, J_1 = 11.7 Hz, J_2 = 2.1 Hz, 2H), 2.88–2.91 (m, 5H), 3.29 (bs, 2H), 3.50 (s, 2H), 3.93 (d, J = 6.3 Hz, 2H), 7.22–7.32 (m, 5H). ^{13}C-NMR ($CDCl_3$): δ 12.84, 28.72, 33.67, 35.45, 43.18, 53.04, 63.17, 69.41, 126.73, 127.93, 128.97, 138.10, 156.11. HRMS (ESI+): *m/z* calcd for $C_{17}H_{27}O_2N_2$ 291.2067; found 291.2066. UPLC purity, 95% at 210 nm (method A, t_R = 2.420 min).

Synthesis of (1-benzylpiperidin-3-yl)methyl ethyl(methyl)carbamate (35)

Synthesized from (1-benzylpiperidin-3-yl)methanol (**51**) (0.201 g, 0.979 mmol, 1.0 equiv.) and *N*-ethyl-*N*-methylcarbamoyl chloride (0.130 mL, 1.175 mmol, 1.2 equiv.) in pyridine (5 mL) via general procedure 2. The crude product was purified by flash column chromatography using CH_2Cl_2/MeOH (20:1, v/v) as the eluent, to produce 0.148 g of **35** as a slightly orange oil (52% yield). R_f = 0.39 (CH_2Cl_2/MeOH, 10:1, v/v). IR (ATR): 2932, 2796, 1698, 1453, 1285, 1174, 1085, 992, 769, 740, 699 cm^{-1}. ^{1}H-NMR ($CDCl_3$): δ 1.00–1.09 (m, 4H), 1.53–1.73 (m, 3H), 1.80 (bs, 1H), 1.92–2.00 (m, 2H), 2.76–2.86 (m, 5H), 3.24 (bd, J = 40.6 Hz, 2H), 3.49 (s, 2H), 3.88 (dd, J_1 = 10.7 Hz, J_2 = 7.5 Hz, 1H), 3.98 (dd, J_1 = 10.5 Hz, J_2 = 5.6 Hz, 1H), 7.21 (m, 5H). ^{13}C-NMR ($CDCl_3$): δ 12.76, 24.48, 26.96, 33.67, 35.86, 43.16, 53.95, 56.72, 63.82, 67.69, 126.64, 127.89, 128.84, 138.26, 155.99. HRMS (ESI+): *m/z* calcd for $C_{17}H_{27}O_2N_2$ 291.2067; found 291.2067. UPLC purity, 97% at 210 nm (method A, t_R = 2.427 min).

Synthesis of 1-(2,3-dihydro-1H-inden-2-yl)piperidin-4-yl ethyl(methyl)carbamate (36)

Synthesized from 1-(2,3-dihydro-1*H*-inden-2-yl)piperidin-4-ol (**52**) (0.200 g, 0.920 mmol, 1.0 equiv.) and *N*-ethyl-*N*-methylcarbamoyl chloride (0.122 mL, 1.104 mmol, 1.2 equiv.) in pyridine (5 mL) via general procedure 2. The crude product was purified by flash column chromatography using CH_2Cl_2/MeOH (20:1, v/v) as the eluent, to produce 0.082 g of **36** as a brown soild (28% yield). R_f = 0.27 (CH_2Cl_2/MeOH, 20:1, v/v). IR (ATR): 2934, 2804, 1699, 1400, 1301, 1179, 1061, 1033, 1021, 741, 619 cm^{-1}. ^{1}H-NMR ($CDCl_3$): δ 1.11 (t, *J* = 7.1 Hz, 3H), 1.77 (bs, 2H), 1.97 (bs, 2H), 2.40 (bs, 2H), 2.76 (bs, 2H), 2.89–2.93 (m, 5H), 3.08 (q, *J* = 7.5 Hz, 2H), 3.17 (q, *J* = 7.6 Hz, 1H), 3.30 (bs, 2H), 4.74 (bs, 1H), 7.12–7.18 (m, 4H). ^{13}C-NMR ($CDCl_3$): δ 12.85, 31.03, 33.76, 37.24, 43.36, 48.93, 66.80, 70.18, 124.24, 126.26, 141.46, 155.55. HRMS (ESI+): *m/z* calcd for $C_{18}H_{27}O_2N_2$ 303.2067; found 303.2067. UPLC purity, 95% at 210 nm (method A, t_R = 2.510 min).

Synthesis of 1-(2,3-dihydro-1H-inden-2-yl)piperidin-3-yl ethyl(methyl)carbamate (37)

Synthesized from 1-(2,3-dihydro-1*H*-inden-2-yl)piperidin-3-ol (**53**) (0.203 g, 0.934 mmol, 1.0 equiv.) and *N*-ethyl-*N*-methylcarbamoyl chloride (0.124 mL, 1.121 mmol, 1.2 equiv.) in pyridine (5 mL) via general procedure 2. The crude product was purified by flash column chromatography using CH_2Cl_2/MeOH (20:1, v/v) as the eluent, to produce 0.089 g of **37** as a brown oil (32% yield). R_f = 0.53 (CH_2Cl_2/MeOH, 15:1, v/v). IR (ATR): 2937, 2794, 1693, 1457, 1400, 1261, 1178, 1118, 1085, 974, 744 cm^{-1}. ^{1}H-NMR ($CDCl_3$): δ 1.10 (t, *J* = 6.8 Hz, 3H), 1.34–1.43 (m, 1H), 1.59–1.69 (m, 1H), 1.74–1.81 (m, 1H), 1.96–2.00 (m, 1H), 2.13–2.18 (m, 2H), 2.75–2.79 (m, 1H), 2.86–2.93 (m, 5H), 3.06 (p, *J* = 7.7 Hz, 3H), 3.14–3.28 (m, 3H), 4.74–4.81 (m, 1H), 7.10–7.18 (m, 4H). ^{13}C-NMR ($CDCl_3$): δ 12.83, 22.93, 30.16, 33.73, 36.86, 36.96, 43.32, 51.26, 55.86, 66.56, 70.16, 124.21, 126.19, 141.46, 155.50. HRMS

(ESI+): *m/z* calcd for $C_{18}H_{27}O_2N_2$ 303.2067; found 303.2066. UPLC purity, 95% at 210 nm (method A, t_R = 2.520 min).

Synthesis of (1-(2,3-dihydro-1H-inden-2-yl)piperidin-4-yl)methyl ethyl(methyl)carbamate (38)

Synthesized from (1-(2,3-dihydro-1*H*-inden-2-yl)piperidin-4-yl)methanol (**54**) (0.202 g, 0.873 mmol, 1.0 equiv.) and *N*-ethyl-*N*-methylcarbamoyl chloride (0.116 mL, 1.048 mmol, 1.2 equiv.) in pyridine (5 mL) via general procedure 2. The crude product was purified by flash column chromatography using CH_2Cl_2/MeOH (15:1, v/v) as the eluent, to produce 0.094 g of **38** as a bown oil (34% yield). R_f = 0.34 (CH_2Cl_2/MeOH, 10:1, v/v). IR (ATR): 2933, 2797, 2752, 1697, 1403, 1284, 1177, 1129, 1087, 985, 745 cm^{-1}. ^{1}H-NMR ($CDCl_3$): δ 1.11 (t, J = 7.2 Hz, 3H), 1.35–1.45 (m, 2H), 1.65–1.78 (m, 3H), 2.05 (td, J_1 = 11.6 Hz, J_2 = 2.0 Hz, 2H), 2.88–2.94 (m, 5H), 3.03–3.11 (m, 4H), 3.14–3.22 (m, 1H), 3.30 (bs, 2H), 3.95 (d, J = 6.3 Hz, 2H), 7.11–7.20 (m, 4H). ^{13}C-NMR ($CDCl_3$): δ 12.91, 28.64, 33.71, 35.44, 36.97, 43.40, 51.30, 66.97, 69.31, 124.16, 126.19, 141.38, 156.07. HRMS (ESI+): *m/z* calcd for $C_{19}H_{29}O_2N_2$ 317.2224; found 317.2223. UPLC purity, 95% at 210 nm (method A, t_R = 2.630 min).

Synthesis of (1-(2,3-dihydro-1H-inden-2-yl)piperidin-3-yl)methyl ethyl(methyl)carbamate (39)

Synthesized from (1-(2,3-dihydro-1*H*-inden-2-yl)piperidin-3-yl)methanol (**55**) (0.202 g, 0.873 mmol, 1.0 equiv.) and *N*-ethyl-*N*-methylcarbamoyl chloride (0.116 mL, 1.048 mmol, 1.2 equiv.) in pyridine (5 mL) via general procedure 2. The crude product was purified by flash column chromatography using CH_2Cl_2/MeOH (20:1, v/v) as the eluent, to produce 0.149 g of **39** as a brown solid (54% yield). R_f = 0.20 (CH_2Cl_2/MeOH, 20:1, v/v). IR (ATR): 2943, 2802, 1702, 1689, 1403, 1299, 1184, 1087, 1007, 749, 524 cm^{-1}. ^{1}H-NMR ($CDCl_3$): δ 0.94–1.08 (m,

1H), 1.11 (t, J = 7.2 Hz, 3H), 1.58–1.69 (m, 1H), 1.72–1.78 (m, 2H), 1.83 (t, J = 10.7 Hz, 1H), 1.99 (td, J_1 = 11.2 Hz, J_2 = 2.3 Hz, 2H), 2.89–2.97 (m, 6H), 3.07 (p, J = 7.5 Hz, 3H), 3.19 (p, J = 8.1 Hz, 1H), 3.29 (bs, 2H), 3.90 (dd, J_1 = 10.3 Hz, J_2 = 7.8 Hz, 1H), 4.01 (q, J = 5.4 Hz, 1H), 7.11–7.19 (m, 4H). ^{13}C-NMR ($CDCl_3$): δ 12.87, 24.67, 27.10, 33.75, 36.02, 36.75, 36.88, 43.25, 51.94, 55.22, 66.99, 67.85, 124.10, 126.11, 141.37, 141.40, 155.95. HRMS (ESI+): *m/z* calcd for $C_{19}H_{29}O_2N_2$ 317.2224; found 317.2223. UPLC purity 97%, at 210 nm (method A, t_R = 2.670 min).

4.4. *In vitro* enzyme inhibition assays

4.4.1. ChE inhibition assay

The inhibitory potencies of the compounds against ChEs were determined using the method of Ellman[38]. 5,5′-Dithiobis (2-nitrobenzoic acid) (Ellman's reagent; DTNB), and the butyrylthiocholine and acetylthiocholine iodides were from Sigma-Aldrich and TCI Europe, respectively. hAChE (stock concentration of 15.0 mg mL^{-1}) and recombinant hBChE (stock concentration of 16.5 mg mL^{-1}) were kindly donated by Xavier Brazzolotto and Florian Nachon (IRBA, Brétigny-sur-Orge, France). The enzyme solutions were prepared by dilution of the concentrated stocks in 0.1 M phosphate-buffered solution, pH 8.0. The reactions were carried out in a final volume of 300 µL of 0.1 M phosphate-buffered solution, pH 8.0, containing 333 µM DTNB, 5 ×10^{-4} M butyrylthiocholine/ acetylthiocholine and 1 ×10^{-9} M or 5 ×10^{-11} M hBChE or hAChE, respectively. The reactions were started by addition of the substrate, at room temperature. The final content of the organic solvent (DMSO) was always 1%. The formation of the yellow 5-thio-2-nitrobenzoate anion as a result of the reaction of DTNB with the thiocholines was monitored for 1 min, as the change in absorbance at 412 nm, using a 96-well microplate reader (Synergy™ H4; BioTek Instruments, Inc., USA). To determine the blank value (b), phosphate-buffered solution replaced the enzyme solution. The

initial velocity (v_0) was calculated from the slope of the linear trend obtained, with each measurement carried out in triplicate. For the first inhibitory screening, stock solutions of the test compounds (10 mM) were prepared in DMSO. The compounds were added to each well at a final concentration of 100 μM. The reactions were started by addition of the substrate to the enzyme and inhibitor that had been preincubated for 30 min, to allow covalent modification of catalytic serine amino-acid residue for irreversible inhibitors to reach complete equilibrium of the enzyme-inhibitor complex. The initial velocities in the presence of the test compounds (v_i) were calculated. The inhibitory potencies are expressed as the residual activities (RA = (v_i – b) / (v_o – b)). For the IC_{50} measurements, seven different concentrations of each compound were used to obtain enzyme activities of between 5% and 90%. The IC_{50} values were obtained by plotting the residual enzyme activities against the applied inhibitor concentrations, with the experimental data fitted to Equation (1):

$$Y = Bottom + (Top - Bottom) / (1+10\hat{}((LogIC_{50} - X) \times HillSlope)) \quad (1),$$

where X is the logarithm of the inhibitor concentration, and Y is the residual activity. For the fitting procedure, the GraphPad Prism 8 (GraphPad Software, USA) was used.

For the reversibility assay, hAChE and hBChE at 100-fold final concentration were incubated with the inhibitors at a concentration 10-fold the IC_{50} at room temperature (volume, 20 μL). After 30 min, 3 μL of the mixture was diluted into 0.1 M phosphate-buffered solution, pH 8.0, containing 507 μM DTNB. The reactions were started by addition of the substrate to the enzyme and inhibitor complex. The final concentrations of all of the reagents and enzymes were the same as in the assay described above. The reaction was monitored for 5 min. Control experiments were carried out in the same manner, where the inhibitor solution was replaced by DMSO. Rivastigmine and donepezil were used as controls.

4.4.2. MAO inhibition assay

The effects of the test compounds on hMAO-A and hMAO-B were investigated using a fluorimetric assay, following a previously described literature method, with minor modifications[39]. The inhibitory activity of the compounds was evaluated by their effects on the production of hydrogen peroxide (H_2O_2) from *p*-tyramine, which was used as a nonspecific substrate for both of these hMAO isoforms. The production of the H_2O_2 was detected using Amplex Red reagent in the presence of horseradish peroxidase, where a highly sensitive fluorescent product, resorufin, is produced at stoichiometric amounts. Recombinant human microsomal hMAO enzymes expressed in baculovirus-infected insect cells (BTI-TN-5B1-4), horse-radish peroxidase (type II, lyophilized powder), and *p*-tyramine hydrochloride were obtained from Sigma Aldrich. 10-Acetyl-3,7-dihydroxyphenoxazine (Amplex Red reagent) was synthesized as described in the literature[44].

Briefly, 100 µL 50 mM sodium phosphate buffer (pH 7.4, 0.05% [v/v] Triton X-114) containing the compounds or the reference inhibitors and hMAO-A or hMAO-B were incubated for 15 min at 37 °C in a flat-bottomed black 96-well microplate (µCLEAR® microplate; Greiner Bio One International GmbH, Germany), and placed in a dark microplate reader chamber. After the pre-incubation, the reaction was started by adding the final concentrations of 250 µM Amplex Red reagent, 2 U/mL horseradish peroxidase, and 1 mM *p*-tyramine (final volume, 200 µL). The production of resorufin was quantified on the basis of the fluorescence generated (λ_{ex} = 530 nm, λ_{em} = 590 nm) at 37 °C over a period of 20 min, during which time the fluorescence increase linearly. For control experiments, DMSO was used instead of the appropriate dilutions of the compounds in DMSO. To determine the blank value (*b*), phosphate-buffered solution replaced the enzyme solution. The initial velocities were calculated from the trends obtained, with each measurement carried out in duplicate. To

obtain the final results the specific fluorescence emission was calculated after subtraction of the blank activity (*b*). The inhibitory potencies are expressed as the residual activities (RA = ($v_i - b$) / ($v_o - b$), where v_i is the velocity in the presence of the test compounds, and v_0 the control velocity in the presence of DMSO. The IC_{50} values were obtained by plotting residual enzyme activities against applied inhibitor concentration, with the experimental data fitted to a Hill four parameter equation (Equation (1)) using GraphPad Prism 8 (GraphPad Software, USA).

For the reversibility assay, hMAO-B at 100-fold final concentration was incubated with the inhibitors at a concentration 10-fold the IC_{50} at 37 °C (volume, 50 µL). After 15 min, the mixture was diluted 100-fold into the reaction buffer containing Amplex Red reagent, horseradish peroxidase, and *p*-tyramine hydrochloride. The final concentrations of all of the reagents and MAO-B were the same as in the assay described above. The reaction was monitored for 30 min. Control experiments were carried out in the same manner, where the inhibitor solution was replaced by DMSO.

4.5. X-ray crystallography of *h*BChE in complex with 13

4.5.1. Crystallization

Recombinant hBChE was produced in eukaryotic cells as described earlier[45] and the protein purified by BChE specific affinity (Hupresin; CHEMFORASE, Rouen, France) followed by size exclusion (Superdex 200, GE Healthcare) chromatographies, as previously described[46]. HBChE crystals were obtained by the hanging drop method at 293 K using a 12 mg/ml protein solution and 0.1 M MES pH 6.5, 2.15 M $(NH_4)_2SO_4$ as crystallization buffer. Compound **13** was solubilized in 100% DMSO at 0.1M concentration and protein complex was obtained by soaking **13** at 1 mM final ligand concentration (0.1 M MES pH 6.5, 2.15 M $(NH_4)_2SO_4$, 1% DMSO). Crystals were cryo-protected in a solution of 0.1 M MES pH 6.5,

2.15 M $(NH_4)_2SO_4$, 20% Glycerol, 1 mM ligand, 1% DMSO before flash cooling into liquid nitrogen.

4.5.2. Structure determination

X-ray diffraction data were collected on the PROXIMA-1 beamline of the SOLEIL Synchrotron (Saint Aubin, France) at 100 K. Images recorded on an EIGER 16M detector were processed with XDS[47]. Data analysis was realized using the Phenix software suite[48]. Initial model was obtained by molecular replacement using Phaser-MR and the hBChE structure (PDB ID 1P0I) devoid of any ligand, glycans or water molecules. Electron density was observed in the active site gorge and allowed unambiguous fitting of the ligand. Ligand geometry restraints were processed with Phenix eLBOW[49] using the semi-empirical quantum mechanical method (AM1). The model was refined by iterative cycles of Phenix.refine and model building using *Coot*[50]. HBChE structure in complex with **13** was deposited into the Protein Data Bank under accession number 6SAM. Figures showing protein structures were generated using the PyMOL software (PyMOL 2.1.1, Schrödinger, NY, USA).

4.6. *In vitro* BBB permeation assay

The *in vitro* permeability through lipid membrane was determined as follows: the compounds were dissolved in DMSO (10 mM stock solution), diluted with 10% (v/v) MeOH in phosphate buffered saline (PBS) buffer (pH 7.4; 0.595 g $Na_2HPO_4 \times 12\ H_2O$, 0.0475 g KH_2PO_4, 2.0 g NaCl in 250 mL deionized water) to 200 µM and transferred in five replicates to the donor 96-well microplate Millipore receiver plate (300 µL/well). The acceptor 96-well Millipore filter plate was coated with 3 µL of lipid solution (PBL 20 mg/mL in hexane/dodecane=3/1 + 1% m/V cholesterol) and prepared with 10 % (v/v) MeOH in PBS buffer (200 µL/well). The acceptor and donor plates were then placed in a »sandwich/contact«

configuration in order to provide contact of lipid filter with the donor solution and left undisturbed for 4 h at 25 °C. After incubation, the plates were separated, well solutions transferred to a UV-plate (UV-Star® Microplate 96 well, half area, µCLEAR®, clear, Ref. 675801, Greiner Bio-One) and concentrations measured using Biotek Synergy HT microplate reader (λ = 230–500 nm in 4 nm steps). Negative logarithm of the effective permeability (–logP_e) was calculated using the in-house software based on A. Avdeef[51]. Assay validation was performed by determining the experimental permeability of five commercial drugs as reference standards and traditional binning used as follows: –logP_e < 5.6, high permeability; –logP_e > 6.2, low permeability; intermediate was labelled as uncertain BBB permeability.

4.7. A$\beta_{1–42}$ aggregation inhibitory activity assay

Thioflavin-T (ThT) fluorometric assay[40]. The inhibition of A$\beta_{1–42}$ aggregation was measured fluorimetrically as described previously[34]. Briefly, HFIP-pretreated A$\beta_{1–42}$ (Merck Millipore, Darmstadt, Germany) at 1.5 µM, the test compound (10 µM final concentration) and Thioflavin-T (10 µM final concentration) were incubated at room temperature in 96-well microplate (covered with aluminum foil to prevent evaporation) with continuous shaking for 36–48 h. The fluorescence intensity (λ_{ex} = 440 nm; λ_{em} = 490 nm) was measured every 3 min (Synergy™ H4 plate reader, BioTek Instruments, Inc. VT, USA). The assay was run in quadruplicates.

4.8. Cell-based assays

4.8.1. Cell culture and treatments

The human neuroblastoma SH-SY5Y cell line was purchased from American Type Culture Collection (CRL-2266, Manassas, VA, USA). The human hepatocellular carcinoma HepG2 cell line was from American Type Culture Collection (HB-8065, LGC Standards,

UK). Cells were cultured in Advanced Dulbecco's modified Eagle's medium (Gibco, Thermo Fisher Scientific, Waltham, MA, USA) supplemented with 10% fetal bovine serum (FBS) (Gibco), 2 mM L-glutamine, 50 U/mL penicillin and 50 µg/mL streptomycin (Sigma, St. Louis, MO, USA) in a humidified atmosphere of 95% air and 5% CO_2 at 37 °C, and grown to 80% confluence. Prior to cell treatment, complete medium was replaced with reduced-serum medium (i.e., with 2% FBS). Compounds **10**, **13**, **16**, **22**, rivastigmine and rasagiline were prepared as a stock solution of 20 mM in DMSO and were used at concentrations of 1 µM to 100 µM. The peptide $A\beta_{1-42}$ (Merck Millipore, Darmstadt, Germany) was dissolved in DMSO at a concentration of 1 mM, and was used as a cytotoxic stimulus at a concentration of 5 µM.

4.8.2. Cell viability assay

To determine the effect of compounds on cell viability, SH-SY5Y and HepG2 cells were seeded in 96-well culture plates (1×10^4/well) and assessed by MTS ([3-(4,5-dimethylthiazol-2-yl)-5-(3-carboxymethoxyphenyl)-2-(4-sulfophenyl)-2*H*-tetrazolium, inner salt) assay. Cells were treated with increasing concentrations (1–100 µM) of test compounds in reduced-serum medium, and cell viability was assessed after 48 h using the CellTiter 96® Aqueous One Solution Cell Proliferation Assay (Promega, Madison, WI, USA), in accordance with the manufacturer's instructions. Absorbance was measured with an automatic microplate reader (Tecan Safire2, Switzerland) at a wavelength of 492 nm. Results are presented as a percentage of the control (DMSO). The LD_{50} values are the mean ± SEM of at least two independent experiments.

4.8.3. Neuroprotection assay

The neuroprotective effect of compounds **10**, **13**, **16**, **22**, rivastigmine and rasagiline on cytotoxic effect of $A\beta_{1-42}$ was determined with the fluorescent intercalator 7-AAD assessed

by flow cytometry. Prior to cell treatment, the peptide $A\beta_{1-42}$ was incubated at final concentration of 5 µM in reduced-serum medium in the absence or presence of compound at concentration 20 µM for 24 h at 37 °C to induce Aβ aggregation. SH-Y5Y cells were seeded in 24-well culture plates (2×10^4/well) and the next day treated with pre-aggregated $A\beta_{1-42}$ in the absence or presence of compounds. After 48 h treatment, cells were harvested, washed in cold PBS, and labelled with 7AAD (2 µg/mL; Sigma Aldrich) for 10 min at room temperature. Cells were then analysed for cytotoxicity by flow cytometry on Attune NxT flow cytometer (Thermo Fisher Scientific). The percentage of 7AAD positive ($7AAD^{pos}$) cells was evaluated using FlowJo software (FlowJo, LLC, Ashland, OR, USA) and recorded as relative to control cells.

4.8.4. Immunofluorescence staining

The SH-SY5Y cells were seeded in complete medium on glass coverslips in 24-well culture plate (2×10^4/mL) in duplicate, and the, next day they were treated with the pre-incubated peptide $A\beta_{1-42}$ (5 µM) in reduced-serum medium in the absence or presence of the compound **10** or compound **16** at 20 µM) for 48 h. The cells were then fixed with 5% formalin in phosphate-buffered saline (PBS), pH 7.4, for 30 min at room temperature, and then permeabilized with 0.5% Tween 20 in PBS for 10 min. Non-specific staining was blocked with 3% bovine serum albumin (BSA) in PBS for 30 min at room temperature. The cells were then incubated with rabbit anti-amyloid fibrils LOC antibody (1:1000; Merck Millipore) in blocking buffer for 2 h at room temperature. Afterwards, the cells were washed with PBS and further incubated with anti-rabbit Alexa Fluor 488-labelled secondary antibodies (1:1000; Thermo Fisher Scientific) in 3% BSA in PBS for an additional 1.5 h. After washing with PBS, the ProLong Antifade kit with DAPI (Molecular Probes, Eugene, OR, USA) was used for mounting the coverslips on glass slides. Fluorescence microscopy

was performed using a Carl Zeiss LSM 710 confocal microscope (Carl Zeiss, Oberkochen, Germany) with the ZEN 2011 image software.

4.8.5. Statistical analyses

The effects of compounds in Neuroprotection assay were analyzed by one-way analysis of variance (ANOVA) and *post-hoc* comparisons were made using *t*-test two-sample equal variances. $P < 0.05$ was considered to be statistically significant. All data are means ± SD.

5. Declaration of competing interest

The authors declare that they have no known competing financial interests or personal relationships that could have appeared to influence the work reported in this paper.

6. Funding

This research was funded by the Slovenian Research Agency (projects Z1-9195, L1-8157 and Z1-1859). Xavier Brazzolotto and Florian Nachon are supported by the French Ministry of Armed Forces (DGA and SSA).

7. Acknowledgements

We thank Ema Valentina Sajovic for performing the HRMS measurements.

8. Abbreviations

7-AAD	7-aminoactinomycin D
Aβ	amyloid β
ACh	acetylcholine
AChE	acetylcholinesterase
AD	Alzheimer's disease
APP	amyloid precursor protein

BBB	blood-brain barrier
BChE	butyrylcholinesterase
BSA	bovine serum albumin
ChE(s)	cholinesterase(s)
DAPI	4′,6-diamidino-2-phenylindole
4-DMAP	*N*,*N*-dimethylpyridin-4-amine
FAD	flavine adenine dinucleotide
hAChE	human acetylcholinesterase
hBChE	human butyrylcholinesterase
hMAO-A	human monoamine oxidase A
hMAO-B	human monoamine oxidase B
mAChE	murine acetylcholinesterase
MAO-A	monoamine oxidase A
MAO-B	monoamine oxidase B
MTDL(s)	multitarget-directed ligand(s)
MTS	**(**3-(4,5-dimethylthiazol-2-yl)-5-(3-carboxymethoxyphenyl)-2-(4-sulfophenyl)-2*H*-tetrazolium, inner salt)
PAMPA	parallel artificial membrane permeation assay
PBS	phosphate buffered saline
PDB	protein data base
SARs	structure–activity relationships

9. Appendix A. Supplementary data

Supplementary data related to this article can be found at

10. References

1. C.L. Masters, R. Bateman, K. Blennow, C.C. Rowe, R.A. Sperling, R. J.L. Cummings, Alzheimer's disease, Nat. Rev. Dis. Primers 1 (2015) 15056.
2. H.W. Querfurth, F.M.N. LaFerla, Engl. J. Med. 362 (2010) 329–344.
3. P. Youssef, B. Chami, J. Lim, T. Middleton, G.T. Sutherland, P.K. Witting, Evidence supporting oxidative stress in a moderately afected area of the brain in Alzheimer’s disease, Sci. Rep. 8 (2018) 11553.
4. M.S. Wolfe, Therapeutic strategies for Alzheimer's disease, Nat. Rev. Drug. Discov. 1 (2002) 859–661.
5. M. Citron, Alzheimer's disease: strategies for disease modification, Nat. Rev. Drug. Discov. 9 (2010) 387–398.

6. P.V. Fisha, D. Steadmana, E.D. Baylea, P. Whitinga, New approaches for the treatment of Alzheimer's disease, Bioorg. Med. Chem. Lett. 29 (2019) 125–133.
7. J. Cummingsa, G. Lee, A. Ritter, M. Sabbagh, K. Zhong, Alzheimer's disease drug development pipeline: 2019, Alzheimers Dement. 5 (2019) 272–293.
8. M.B.H.Youdim, D. Edmondson, K.F. Tipton, The therapeutic potential of monoamine oxidase inhibitors, Nat. Rev. Neurosci. 7 (2006) 295–309.
9. C. Binda, P. Newton-Vinson, P., F. Hubálek, D.E. Edmondson, A. Mattevi, Structure of human monoamine oxidase B, a drug target for the treatment of neurological disorders, Nat. Struct. Mol. Biol. 9 (2002) 22–26.
10. S. Carradori, R. Silvestri, New frontiers in selective human MAO-B inhibitors, J. Med. Chem. 58 (2015) 6717–6732.
11. E. Scherder, Aging and dementia: neuropsychology, motor Skills, and pain, 1st ed; VU University Press, Amsterdam, 2011, pp. 9–32.
12. E. Scarpini, P. Schelterns, H. Feldman, Treatment of Alzheimer's disease: current status and new perspectives, Lancet Neurol. 2 (2003) 539−547.
13. E.K. Perry, B.E. Tomlinson, G. Blessed, K. Bergmann, P.H. Gibson, R.H. Perry, Correlation of cholinergic abnormalities with senile plaques and mental test scores in senile dementia, Br. Med. J. 2 (1978) 1457–1459.
14. A. Chatonnet, O. Lockridge, Comparison of butyrylcholinesterase and acetylcholinesterase, Biochem J. 260 (1989) 625–634.
15. P.E. Lee, G.Y.R. Hsiung, D. Seitz, S.S. Gill, P.A. Rochon, Cholinesterase inhibitors, B. C. Med. J. 53 (2011) 404–408.
16. R.M. Lane, S.G. Potkin, A. Enz, Targeting acetylcholinesterase and butyrylcholinesterase in dementia, Int. J. Neuropsychopharmacol. 9 (2006) 101–124.

17. H. Sugimoto, Y. Iimura, Y. Yamanishi, K. Yamatsu, Synthesis and structure-activity relationships of acetylcholinesterase inhibitors: 1-benzyl-4-[(5,6-dimethoxy-1-oxoindan-2-yl)methyl]piperidine hydrochloride and related compounds, J. Med. Chem. 38 (1995) 4821−4829.
18. H.M. Greenblatt, G. Kryger, T. Lewis, I. Silman, J.L. Sussman, Structure of acetylcholinesterase complexed with (−)-galanthamine at 2.3 A resolution. FEBS Lett. 463 (1999) 321−326.
19. P. Bar-On, C.B. Millard, M. Harel, H. Dvir, A. Enz, J.L. Sussman, I. Silman, Kinetic and structural studies on the interaction of cholinesterases with the anti-Alzheimer drug rivastigmine, Biochemistry 41 (2002) 3555−3564.
20. M.G. Savelieff, G. Nam, J. Kang, H.J. Lee, M. Lee, M.H. Lim, Development of multifunctional molecules as potential therapeutic candidates for Alzheimer's disease, Parkinson's disease, and amyotrophic lateral sclerosis in the last decade, Chem. Rev. 119 (2019) 1221−1322.
21. D. Knez, M. Sova, U. Košak, S. Gobec, Dual inhibitors of cholinesterases and monoamine oxidases for Alzheimer's disease, Future Med. Chem. 9 (2017) 811–832.
22. H. Wang, H. Zhang, Reconsideration of anticholinesterase therapeutic strategies angainst Alzheimer's disease, ACS Chem. Neurosci. 10 (2019) 852–862.
23. O. Weinreb, T. Amit, O. Bar-Am O, M.B. Youdim, Ladostigil: a novel multimodal neuroprotective drug with cholinesterase and brain-selective monoamine oxidase inhibitory activities for Alzheimer's disease treatment. Curr. Drug Targets. 13 (2012) 483–94.
24. L. Li, S. Xu, L. Liu, R. Feng, Y. Gong, X. Zhao, J. Li, J. Cai, N. Feng, L. Wang, X. Wang, Y. Peng, Multifunctional compound AD-35 improves cognitive impairment and

attenuates the production of TNF-α and IL-1β in an Aβ25-35-induced rat model of Alzheimer's disease, J. Alzheimers Dis. 56 (2017) 1403–1417.

25. L.S. Schneider, Y. Geffen, J. Rabinowitz, R.G. Thomas, R. Schmidt, S. Ropele, M. Weinstock, Low-dose ladostigil for mild cognitive impairment: a phase 2 placebo-controlled clinical trial. Neurology 93 (2019) 1474–1484.
26. J.L. Cummings, T. Morstorf, K. Zhong, Alzheimer's disease drug-development pipeline: few candidates, frequent failures, Alzheimers Res. Ther. 6 (2014) 37.
27. B. Brus, U. Košak, S. Turk, A. Pišlar, N. Coquelle, J. Kos, J. Stojan, J.P. Colletier, S. Gobec, Discovery, biological evaluation, and crystal structure of a novel nanomolar selective butyrylcholinesterase inhibitor, J. Med. Chem. 57 (2014) 8167−8179.
28. U. Košak, B. Brus, D. Knez, R. Šink, S. Žakelj, J. Trontelj, A. Pišlar, J. Šlenc, M. Gobec, M. Živin, L. Tratnjek, M. Perše, K. Sałat, A. Podkowa, B. Filipek, F. Nachon, X. Brazzolotto, A. Więckowska, B. Malawska, J. Stojan, I. Mlinarič Rasčan, J. Kos, N. Coquelle, J.P. Colletier, S. Gobec, Development of an in-vivo active reversible butyrylcholinesterase inhibitor. Sci. Rep. 6 (2016) 39495.
29. U. Košak, B. Brus, D. Knez, S. Žakelj, J. Trontelj, A. Pišlar, R. Šink, M. Jukić, M. Živin, A. Podkowa, F. Nachon, X. Brazzolotto, J. Stojan, J. Kos, N. Coquelle, K. Sałat, J.P. Colletier, S. Gobec, The magic of crystal structure-based inhibitor optimization: development of a butyrylcholinesterase inhibitor with picomolar affinity and in vivo activity. J. Med. Chem. 61 (2018) 119–139.
30. C. Binda, F. Hubálek, M. Li, Y. Herzig, J. Sterling, D.E. Edmondson, A. Mattevi, Crystal structures of monoamine oxidase B in complex with four inhibitors of the *N*-propargylaminoindan class, J. Med. Chem. 47 (2004) 1767–1774.
31. Q.S. Yu, X.F. Pei, H.W. Holloway, N.H. Greig, A. Brossi, Total syntheses and anticholinesterase activities of (3a*S*)-*N*(8)-norphysostigmine, (3a*S*)-*N*(8)-

norphenserine, their antipodal isomers, and other *N*(8)-substituted analogues, J. Med. Chem. 40 (1997) 2895–2901.

32. Q.S. Yu, H.W. Holloway, T. Utsuki, A. Brossi, N.H. Greig, Synthesis of novel phenserine-based-selective inhibitors of butyrylcholinesterase for Alzheimer's disease, J. Med. Chem. 42 (1999) 1855–1861.
33. C. Bartolucci, J. Stojan, Q. Yu, N.H. Greig, D. Lamba, Kinetics of *Torpedo californica* acetylcholinesterase inhibition by bisnorcymserine and crystal structure of the complex with its leaving group, Biochem. J. 444 (2012) 269–277.
34. U. Košak, D. Knez, N. Coquelle, B. Brus, A. Pišlar, F. Nachon, X. Brazzolotto, J. Kos, J.P. Colletier, S. Gobec, *N*-propargylpiperidines with naphthalene-2-carboxamide or naphthalene-2-sulfonamide moieties: potential multifunctional anti-Alzheimer's agents. Bioorg. Med. Chem. 25 (2017) 633–645.
35. M. Prokopowicz, P. Mlynarz, P. Kafarski, Synthesis of phosphonate derivatives of 2,3-dihydroindene, Tetrahedron Lett. 50 (2009) 7314–7317.
36. C. Stock, R. Brückner, Exceptionally active catalysts for the formation of carbamates from alcohols and isocyanates: molybdenum(VI) dichloride dioxide and its dMF complex, Synlett 16 (2010) 2429–2434.
37. R.F. Atkinson, T.W. Balko, T.R. Westman, G.C. Sypniewski, M.A. Carmody, C.T. Pauler, C.L. Schade, D.E. Coulter, H.T. Pham, F. Barea, Formation of olefins in the pyrolysis of *N*,*N*-disubstituted carbamates, J. Org. Chem. 46 (1981) 2804–2806.
38. G.L. Ellman, K.D. Courtney, V. Andres jr., R.M. Featherstone, A new and rapid colorimetric determination of acetylcholinesterase activity, Biochem. Pharmacol. 7 (1961) 88–95.
39. O.M. Bautista-Aguilera, A. Samadi, M. Chioua, K. Nikolic, S. Filipic, D. Agbaba, E. Soriano, L. de Andrés, L.; M.I. Rodríguez-Franco, S. Alcaro, R.R. Ramsay, F. Ortuso,

M. Yañez, J. Marco-Contelles, *N*-methyl-*N*-((1-methyl-5-(3-(1-(2-methylbenzyl)piperidin-4-yl)propoxy)-1*H*-indol-2-yl)methyl)prop-2-yn-1-amine, a new cholinesterase and monoamine oxidase dual inhibitor, J. Med. Chem. 24 (2014) 10455–10463.

40. H. LeVine 3rd, Thioflavine T interaction with synthetic Alzheimer's disease beta-amyloid peptides: detection of amyloid aggregation in solution, Protein Sci. Publ. Protein Soc. 2 (1993) 404–410.
41. Z. Rankovic, CNS drug design: balancing physicochemical properties for optimal brain exposure, J. Med. Chem. 58 (2015) 2584–2608.
42. S. Jin, N. Kedia, E. Illes-Toth, I. Haralampiev, S. Prisner, A. Herrmann, E.E. Wanker, J. Bieschke, Amyloid-β(1-42) aggregation initiates its cellular uptake and cytotoxicity. J. Biol. Chem. 291 (2016) 19590–19606.
43. A.K. Ghosh, M. Brindisi, Organic carbamates in drug design and medicinal chemistry, J. Med. Chem. 58 (2015) 2895–2940.
44. H. Von der Eltz, H.J. Guder, K. Muhlegger, USP Patent No. 4900822, Feb. 13, 1990.
45. N. Florian, Y. Nicolet, N. Viguié, P. Masson, J.C. Fontecilla□Camps, O. Lockridge, Engineering of a monomeric and low-glycosylated form of human butyrylcholinesterase: expression, purification, characterization and crystallization, Eur. J. Biochem., 269 (2002) 630–637.
46. X. Brazzolotto, M. Wandhammer, C. Ronco, M. Trovaslet, L. Jean, O. Lockridge P.Y. Renard, F. Nachon, Human butyrylcholinesterase produced in insect cells: huprine-based affinity purification and crystal structure. FEBS J., 279 (2012) 2905–2916.
47. W. Kabsch, *XDS.* Acta Crystallogr. D. Biol. Crystallogr. 66 (2010) 125–132.

48. P.D. Adams, P.V. Afonine, G. Bunkóczi, V.B. Chen, I.W. Davis, N. Echols, J.J. Headd, L.W. Hung, G.J. Kapral, R.W. Grosse-Kunstleve, A.J. McCoy, N.W. Moriarty, R. Oeffner, R.J. Read, D.C. Richardson, J.S. Richardson, T.C. Terwilliger and P.H. Zwart, PHENIX: a comprehensive Python-based system for macromolecular structure solution, Acta Crystallogr. D. Biol. Crystallogr., 66 (2010) 213–221.

49. N.W. Moriarty, R.W. Grosse-Kunstleve, P.D. Adams, electronic Ligand Builder and Optimization Workbench (eLBOW): a tool for ligand coordinate and restraint generation. Acta Crystallogr. D. Biol. Crystallogr., 65 (2009) 1074–1080.

50. P. Emsley, B. Lohkamp, W.G. Scott. K. Cowtan, Features and development of Coot, Acta Crystallogr. D. Biol. Crystallogr., 66 (2010) 486–501.

51. A. Avdeef, Absorption and Drug Development: Solubility, Permeability, and Charge State, 2nd ed; John Wiley & Sons, Hoboken, N.J., 2012.

Highlights

- Novel *N*-alkylpiperidine carbamates were designed, synthesised and bioevaluated.
- Compound **10** inhibits cholinesterases, monoamine oxidase B and is neuroprotective.
- Compound **13** is a potent selective butyrycholinesterase inhibitor.
- Neuroprotective compound **16** inhibits monoamine oxidase B and amyloid β aggregation.
- Compound **22** inhibits both acetylcholinesterase and butyrylcholinesterase.

Declaration of interests

☒ The authors declare that they have no known competing financial interests or personal relationships that could have appeared to influence the work reported in this paper.

☐The authors declare the following financial interests/personal relationships which may be considered as potential competing interests: